

**Seismic Assessment and Retrofitting of an Existing
RC Building by Shear Walls Constructed with
Mixture of Crushed Waste Tires Rubber**

Abdullah R. M. Alariyan

Submitted to the
Institute of Graduate Studies and Research
in partial fulfillment of the requirements for the degree of

Master of Science
in
Civil Engineering

Eastern Mediterranean University
December 2019
Gazimağusa, North Cyprus

Approval of the Institute of Graduate Studies and Research

Prof. Dr. Ali Hakan Ulusoy
Acting Director

I certify that this thesis satisfies all the requirements as a thesis for the degree of Master of Science in Civil Engineering.

Assoc. Prof. Dr. Serhan Şensoy
Chair, Department of Civil Engineering

We certify that we have read this thesis and that in our opinion it is fully adequate in scope and quality as a thesis for the degree of Master of Science in Civil Engineering.

Assoc. Prof. Dr. Mehmet Cemal
Geneş
Supervisor

Examining Committee

1. Assoc. Prof. Dr. Mehmet Cemal Geneş

2. Asst. Prof. Dr. Mohammed Ali Mosaberpanah

3. Asst. Prof. Dr. Eriş Uygur

ABSTRACT

The seismic actions that happen in Turkey and some other neighboring countries puts the region in great danger. Also, a variety of soil conditions can amplify ground motions in different ways. Over the past 20 years, both scientists and engineers began to study available structures and the ways they can resist their lateral loading potential, earthquake hazard, and vulnerability. These structures can be adjusted to incorporate new techniques and improvements to oppose quake and seismic burdens, which are considered the most critical source of financial and social disaster in urban areas. This thesis introduces a case study on strengthening a five-story reinforced concrete structure with RC shear walls constructed using waste crushed rubber that was built in 1988 and is located in Antakya, Turkey. This work consists of three stages. First, collecting data, which included building plans, material properties that were determined using a non-destructive testing method called the forced vibration test, structural condition, and reinforcement details. In the second stage, the model calibration was done by modeling a structure with dominant periods and mode shapes similar or identical to the existing building, which were determined using forced vibration tests. A nonlinear static pushover analysis of the model was conducted to evaluate its seismic performance according to the procedures outlined in ATC-40. In the third step, the existing building that showed low performance based on the code requirements has been strengthened using shear walls constructed with waste crushed rubber. Several different shear wall locations were tested to determine the most appropriate configuration. The shear walls have been attached to the building in a Y-direction to both sides of the building which have poor

performance. It is emphasized that this strengthening technique is an appropriate method according to the performance and cost analysis.

Keywords: Earthquake Evaluation, Pushover analysis, Strengthening, Forced vibration test

ÖZ

Türkiye'de ve diğer bazı komşu ülkelerde gerçekleşen sismik hareketler, bölgeyi büyük bir tehlikeye sokmaktadır. Ayrıca, çeşitli zemin koşulları, farklı yer hareketi büyütmelerine neden olmaktadır. Son 20 yıl boyunca, hem bilim adamları hem de mühendisler mevcut yapıları ve bu yapıların yanal yüklere karşı koyma potansiyellerini, deprem hasarlarını ve hasar görülebilirliklerini incelemektedirler. Bu yapılar, kentsel alanlarda en kritik finansal ve sosyal felaket olarak kabul edilen deprem ve sismik yüklere karşı yeni teknikleri ve iyileştirmeleri içerecek şekilde ayarlanabilirler. Bu tez, 1988 yılında inşa edilmiş ve Antakya'da bulunan beş katlı betonarme bir yapının, atık kırma kauçuk katkısı ile inşa edilecek olan betonarme perde duvarları ile güçlendirilmesine yönelik bir çalışmayı sunmaktadır. Bu çalışma üç aşamadan oluşmaktadır. İlk aşama, bina planlarını, zorlanmış titreşim denilen tahribatsız test yöntemi kullanılarak varsayılan malzeme özelliklerinin tespit edilmesini, yapısal durumunun test edilmesi ve donatı detaylarını içeren veri toplama aşamasıdır. İkinci aşama, model kalibrasyonu, modellenen yapının, mevcut binanın zorlanmış titreşim testleri kullanılarak ölçülmüş olan baskın periyot ve mod şekillerine benzer veya yakın olacak şekilde modellenmesiyle yapılmıştır. Model kalibrasyonundan sonra, ATC-40 yöntemlerine dayanan sismik performans değerlendirmesi için doğrusal olmayan statik itme analizi yapılmıştır. Son olarak, yönetmelik gereksinimlerine göre düşük performans gösteren mevcut bina, atık parçalanmış kauçuk katkısı ile yapılmış perde duvarları kullanılarak güçlendirilmiştir. En uygun güçlendirimin bulunması için birkaç farklı perde duvar yeri denenmiştir. Binanın düşük performans gösterdiği Y-yönünde binanın her iki

tarafında simetriyi sađlayacak řekilde eklenmiřlerdir. Bu gçlendirme tekniđinin performans ve maliyet analizine gre uygun bir yntem olduđu vurgulanmıřtır.

Anahtar Kelimeler: Deprem Deđerlendirmesi, Statik itme analizi, Gçlendirme, Zorlanmıř titreřim deneyi

DEDICATION

To My Family

My Father and My Mother

My Brother and Sisters

My Friends and Teachers

ACKNOWLEDGEMENT

I would never have been able to finish my dissertation without the guidance of my committee members, help from friends, and support from my family.

I would like to express my deepest gratitude to my advisor, Assoc. Prof. Dr. Mehmet Cemal Genç, for his excellent guidance, care, patience, and providing me with an excellent atmosphere for doing research. Likewise, I would like to thank my teacher Mr. Walid Hasan for his motivation. Thanks are also due to all the members of the examining committee and all other members of the Department of Civil Engineering at Eastern Mediterranean University (EMU).

I would like to thank my parents, Mr. Riyadh Alariyan and Mrs. Najah Dohan, my brother, my sisters and all my friends, I thank you for your endless prayers and encouragement. I appreciate all of the times you visited, called, chatted and e-mailed with words of faith, encouragement, and wisdom that carried me through every day of this process. Thanks to all that encouraged me to complete my study.

Finally, I would like to express my appreciation to everyone who made these years in Cyprus a wonderful experience. Thanking in advance.

TABLE OF CONTENTS

ABSTRACT.....	iii
ÖZ.....	v
DEDICATION.....	vii
ACKNOWLEDGEMENT.....	viii
LIST OF TABLES.....	xii
LIST OF FIGURES.....	xiv
LIST OF SYMBOLS AND ABBREVIATIONS.....	xvi
1 INTRODUCTION.....	1
1.1 Overview.....	1
1.2 Problem Statement.....	7
1.3 Thesis Objectives.....	7
1.4 Content of Thesis.....	8
2 LITERATURE REVIEW.....	10
2.1 Studies on Mechanical Properties of Crushed Rubber Waste Tires.....	12
2.1.1 Tensile Strength.....	13
2.1.2 Compressive Strength.....	13
2.1.3 Flexural Failure.....	15
2.1.4 Flexural Strength.....	16
2.1.5 Shear Failure.....	16
2.2 Risk of Earthquake.....	18
2.3 Building Resilience.....	19
2.4 Methods for Modelling Seismic Performance.....	21
2.5 Strengthening Techniques for RC Buildings.....	23

2.5.1 Strengthening Techniques Base on Strengthening of Building Connection	25
2.5.2 Strengthening Techniques Based on Improving Structural Systems	29
2.6 Past Studies on Pushover Analysis	33
3 METHODOLOGY AND DATA COLLECTION	35
3.1 Introduction	35
3.2 Research Methodology	35
3.3 Data Collection	38
3.3.1 Information About the Building Under Study	38
3.3.2 Building Details	38
3.3.3 Material Properties of the Building	40
3.3.4 Modeling of Infill Walls	43
3.3.5 Modeling the Building and Model Calibration the Building	45
3.4 Seismic Assessment of the Building	46
3.4.1 The Capacity Spectrum and Demand Spectrum	46
3.4.2 Displacement Coefficient Methodology (FEMA 356)	48
3.4.3 Performance Levels of Building	49
3.4.4 Nonlinear Plastic Hinge Properties	51
3.4.5 Pushover Analysis Applications in SAP2000	52
3.5 Performance-Based Earthquake Engineering	55
3.5.1 Nonlinear Static Analysis Procedure (Pushover Analysis)	55
3.5.2 Capacity Spectrum Method (CSM), (ATC 40)	55
3.5.3 Nonlinear Static Pushover Analysis of the MDOF Model	56
3.5.5 Conversion of Capacity Curve to Capacity Spectrum	57

3.5.6 Superposition of the Capacity Spectrum on the Elastic Damped Demand Spectrum	58
3.5.7 Equivalent Viscous Damping.....	59
3.5.8 Performance Point of Equivalent SDOF System	59
3.5.9 Performance Point of MDOF System	59
3.6 Strengthening the Building Using Shear Wall with Crushed Waste Tires	60
4 RESULTS AND DISCUSSION	63
4.1 Introduction	63
4.2 Details of the Modelling	64
4.3 Model Calibration	65
4.4 Performance of the Building Before Strengthening.....	66
4.5 Performance of the Building After Strengthening	74
4.5.1 Strengthening by Shear Wall	74
4.5.2 Performance in X-Direction after Strengthening	76
4.5.3 Performance in Y-Direction after Strengthening	78
4.6 Comparative Demand and Capacity Spectrum for X and Y-Direction Before and After Strengthening	81
4.7 Comparison of the Cost Estimations Between Different Types of Concrete Mixtures Including Waste Tire Rubber.....	82
5 CONCLUSION AND RECOMMENDATIONS.....	84
5.1 Summary	84
5.2 Conclusion	85
5.3 Recommendations for Further Studies.....	86
REFERENCES.....	87
APPENDIX.....	97

LIST OF TABLES

Table 3.1: Vibration frequencies and periods.	45
Table 3.2: Existing properties and code parameters of the building.....	53
Table 3.3: Mix identifications and proportions of materials.....	61
Table 3.4: Mechanical properties of concrete replaced with waste rubber.....	62
Table 4.1: Details of the model.....	64
Table 4.2: Period and frequency of the model	66
Table 4.3: Plastic hinges state in X-direction before strengthening.....	69
Table 4.4: Plastic hinges state in Y-direction before strengthening.....	70
Table 4.5: Immediate occupancy performance level in X-direction for beams in existing structure.	72
Table 4.6: Immediate occupancy performance level in X-direction for columns in existing structure.	73
Table 4.7: Immediate occupancy performance level in Y-direction for beams in existing structure.	73
Table 4.8: Immediate occupancy performance level in Y-direction for columns in existing structure.	73
Table 4.9: Performance points for frames with and without shear walls (X-Direction).	76
Table 4. 10: Hinges states before and after strengthening in X direction	77
Table 4.11: Performance points for both of frames with and without shear wall (Y-Direction)	78
Table 4.12: Hinges states in Y direction	79
Table 4.13: Cost price of the first shear wall configurations	82

Table 4.14: Cost price of the second shear wall congregation.....	83
Table 4.15: Cost price of the third shear wall configurations	83

LIST OF FIGURES

Figure 1.1: Monotonic loading with perfect plastic structure.....	3
Figure 2.1: Compressive strength against rubber cement (Khatib and Bayomy, 1999)..	14
Figure 2. 2: Description of Shear failure.....	17
Figure 2.3: Flow of seismic inertia forces during through structural components (Kaplan, et al.2011).....	24
Figure 2.4: Reinforced concrete jacketing (source: DEPTA Engineering).....	25
Figure 2.5: Using steel jacketing for connection (Source: RADYAB Engineering Solution).....	29
Figure 2.6: Application of infill shear wall in RC building (Baran, 2005).....	31
Figure 2.7: External steel bracing frame out of a structure (Prakash and Thakkar, 2003).	33
Figure 3.1: Analysis of the existing building.....	37
Figure 3.2: Location of studied apartment in Antakya, Turkey.....	38
Figure 3.3: Studied apartment view in Antakya, Turkey.....	39
Figure 3.4: The shaker.....	41
Figure 3.5: Sensors by syscom.....	42
Figure 3.6: Layout of the building accelerometer sensors and vibration generator...	43
Figure 3.7: Modeling of brick infill wall as equivalent pressure strut.....	44
Figure 3.8: Demand and capacity spectrum (Vijayakumar et al., 2012).	47
Figure 3.9: Different stages and definition of plastic hinge (Vijayakumar, et al. 2012).	51
Figure 3.10: Three dimensional model of the building.....	52

Figure 3.11: Default hinge properties of the frame.....	53
Figure 3.12: Bilinear approximation of the capacity curve.....	57
Figure 3.13: Initial estimation of performance point using the Equal Displacement rule.....	58
Figure 3.14: Estimation of target displacement using CSM method	59
Figure 3.15: Infill shear wall (Akin, et al., 2016).	62
Figure 3.16: Reinforcement distribution in the shear wall.....	62
Figure 4.1: Demand and capacity spectrum in X-direction before strengthening.....	67
Figure 4.2: Demand and capacity spectrum in Y-direction before strengthening	68
Figure 4.3: Hinges state in step 16 in X-direction	71
Figure 4.4: Hinges states in step 23 Y-direction	71
Figure 4.5: First shear wall configuration used for strengthening (shear wall-I)	74
Figure 4.6: Second shear wall configuration used for strengthening (shear wall-II)...	75
Figure 4.7: Their shear wall congregation used for strengthening (shear wall-III)	75
Figure 4.8: Hinges states in step 14 in X direction	77
Figure 4.9: Hinges states in step 12 in Y-direction.....	79

LIST OF SYMBOLS AND ABBREVIATIONS

A_o	Seismic Zone Factor
C_0	The coefficient correlating the displacement
C_1	Modification factor to relate expected maximum inelastic displacements to displacements
C_2	Modification factor to represent the effect of pinched hysteretic shape, stiffness degradation and strength deterioration on maximum displacement response.
C_3	Modification factor to represent increased displacements due to dynamic P- Δ effects.
C_m	Effective mass factor to take in the account the higher mode mass participation effects obtained from Table 3-1 in FEMA 356.
E_c	Modulus of elasticity of concrete
f'_c	Cylinder Characteristic Compression Strength of Concrete
g	Acceleration of gravity
I	Building Importance Factor
S_a	Response spectrum acceleration, at the effective fundamental period and damping ratio of the building in the direction under consideration, g
T_e	Effective fundamental period of the building in the direction under consideration
V_t	Target shear force
W	Total building weight
δt	Target displacement

25RBC	25% Rubberized Concrete
ADRS	Acceleration versus Displacement Response Spectrum
ADRS	Accelerated-displacement response spectrum
RCZ	Reinforced concrete jacketing
ASCE	American Society Of Civil Engineers
ATC	Applied Technology Council (Seismic evaluation and retrofit of concrete buildings)
CP	Collapse Prevention
CSM	Capacity Spectrum Method
FCR	Fine crumb rubber
FEMA	Federal Emergency Management Agency
IO	Immediate Occupancy
LS	Life Safety
NCC	Network Control Centre
PRC	Precast reinforced concrete
RC	Reinforced Concrete
TC	Tire chips
TEC	Turkish Earthquake Code
TRAC	Tire rubber aggregate concrete
TSC	Turkish Standard Code

Chapter 1

INTRODUCTION

1.1 Overview

Earthquakes are one of Earth's complex phenomenon. They are the result of a shift in plate of the Earth's crust or plate tectonics. It occurs when the frictional stress of a gliding plate builds, causing failure at the fault line. The results of earthquakes are evident globally, including loss of lives and properties. In Turkey, an earthquake of magnitude 7.7 struck Kocaeli in 1999. Casualties of about 17,000 were recorded with about 44,000 injured. Emergency housing for about 25,000 people required 121,000 tents. The damage included the destruction of about 214,000 residential buildings and around 30,500 business buildings.

Turkey is located in a highly active earthquake zone. This requires buildings to adhere to the 2007 Turkish Earthquake Code (TEC). Moreover, an updated Turkish Earthquake Code (TEC) was published in 2018. This code ensures the safety of structures. However, it has been noted that most residential structures constructed before 1998 are designed without adequate details and reinforcement for seismic performance. The absence of this increases the probability of a catastrophic collapse.

Parameters that influence the level of earthquake damage include the duration and frequency of ground motion, intensity, construction quality, and the condition of the

soil. Population density and the period the earthquake occurs are sociological factors that also influence the level of earthquake damage.

Buildings designed before 1998 followed the dated TEC i.e. TEC 1984 and TEC 1975, which are invalid today. Due to cost efficiency and the time associated with the evaluation and strengthening of buildings, it is important to have a quick, effective and cost-efficient method for buildings that follow the dated TEC requirements. An evaluation of the building is used to strengthen the structure of the building. The strengthening is applied if the cost is less than 40% of the building's appraisal cost.

The structural strengthening design should be as follows:

- Lateral load resistance to earthquake
- Enhancement of building rigidity to withstand ground acceleration
- Guarantee of an excellent strengthening system
- The ductility of the building should be reviewed to decrease seismic action.

Ductility refers to a building's ability to experience significant deformation without collapse. Figure 1.1 illustrates the plastic structure of monotonic loading.

The goal of any strengthening method is supporting the building so that its displacement does not exceed its capacity (Kaplan et al., 2011). The reinforcement can be achieved either by reducing the expected displacement of the whole structure system or increasing the structural system capacity by providing ductility to the building.

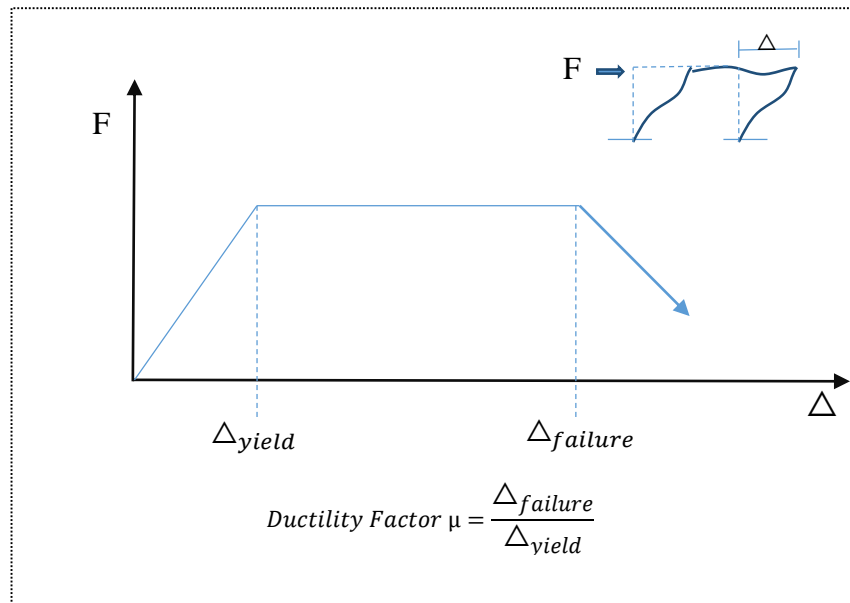


Figure 1.1: Monotonic loading with perfect plastic structure.

Once the performance level and properties of the building are determined, structural reinforcement can be undertaken to increase the building's resistance against seismic activities. In this process, a proper structural strengthening technique must be implemented for the particular building with the consideration of earthquake and seismic specifications.

The seismic design for buildings is determined by the TEC 2007 and Turkish Building Seismic Code (2018) (TBSC 2018) requirements. It suggests the factors to be considered during structural design. The recommended factors are as follows:

- Minimum damages should be observed during minor earthquakes (structural and non-structural damages).
- Moderate earthquakes should produce no structural damages. However, non-structural damages are reasonably expected.

- Structural collapse should be prevented in severe earthquake situation. However, the occurrence of structural and non-structural damages is expected.

In old structural designs, seismic actions and factors were not considered. Therefore, performance evaluations must be performed on existing buildings. This is done in two stages. Stage one involves building conditions and data collection. Stage two involves the assessment of performance levels, which are categorized into three groups depending on the level of severity: immediate occupancy, life safety, and collapse prevention.

The evaluation of structural performance can be performed using different methods. However, in this thesis, we will be applying only the nonlinear static method commonly known as “Pushover”. This is a simplification of the nonlinear seismic response spectrum analysis. The procedure is carried out as follows: the simulated lateral forces are inserted into the model, followed by a step by step ramping to the target displacement where the structural seismic behavior is evaluated. The methodology chapter provides a detailed description of this process.

After determining the properties and performance level of the building, the structural reinforcement can be implemented to improve/increase the resistance of the building to seismic activities. To achieve this, an adequate structural strengthening strategy must be chosen for the individual building, taking into consideration the seismic and earthquake specifications. A method for strengthening by adding shear walls is proposed by Onat et al., (2018). Some advantages of this method include minimum interference with the tenants of the building, cost-effectiveness, environmental

friendliness, and sustainability. Performance factors that must be considered during strengthening of existing buildings include: aesthetic plastering, preventing the loss of substrates, and shielding reinforcement.

The amount of waste tires is growing exponentially around the world. About 247 million waste tires are produced in the USA alone. It is estimated that about 1.5 billion waste tires are produced around the world annually. In Turkey, studies from the field of waste management have shown a drastic rise in waste tire disposal. Environmental friendly methods of waste tire disposal are being promoted.

The use of waste tire rubber as an aggregate in concrete has grown significantly over the last couple of decades. They are used either as a substitute or complete replacement of the aggregate in a concrete mixture (Marie and Quiasrawi, 2012; Su et al., 2015).

The workability of concrete containing rubber is known to be lesser than those that don't (Khatib et al., 1999; Oikonomou et al., 2009). A high deposit of tires is known to have environmental and economic risks. Researchers have found that the combination of rubber and concrete decreases the compressive strength of concrete (Eldin and Senouci, 1993; Topçu, 1997). Previous studies on the application of tire rubber particles are mostly concentrated on cement-based materials and its utilization as a coarse aggregate in concrete. The mechanical properties are typically evaluated and most results show a decrease in density, increase in ductility and toughness, reduction in splitting tensile strength and compressive strength with an improvement in insulation.

The impact of using the scrap tire rubber aggregate as a partial replacement for natural aggregates, on compressive, tensile and flexural strengths, has been well documented. A large number of studies, including Eldin and Senouci,(1993), Toutanji, (1996), and Naik (2004), have reported that the compressive/tensile strength and static modulus of elasticity for precast reinforced concrete (PRC) decreases significantly with increased quantities of rubber.

In producing the shear walls, crushed rubber is used in the aggregate. The aggregate serves as a reinforcement to add tensile strength to the overall composite material. These aggregates tend to change its physical and mechanical characteristics, dimensions, treatment, and possible separations depending on the type of tires used. This is an achievable direction for great advancement in the field of civil engineering. The potential of using rubber from worn tires in many civil engineering works has been studied over the last couple of decades (Shu and Huang, 2014). Applications where tires can be used and where the addition of tire rubber has proven to be effective in protecting the environment and conserving natural resources include the production of cement mixtures, road construction, geotechnical works and reinforcing concrete (Shu and Huang, 2014). Tires are traditionally dumped carelessly and landfilled, ignoring their great importance. Rubber from these scrap tires happen to be one of the most recent waste materials recognized by engineers for its potential use in the engineering field and has increased the level of advancement in all engineering sectors. This thesis investigates an existing RC building to retrofit and strengthen it by using shear walls constructed with a mixture of crushed waste tires rubber.

1.2 Problem Statement

Many structures in Turkey do not follow the TEC 2007 and the new code TBSC 2018, which are important construction guidelines. Disregard for these codes can lead to catastrophic collapse during earthquakes or other disastrous activities. A significant amount of house owners cannot afford the cost implications of the current evaluation and strengthening process. Thus, there is a need for a fast and cost-effective way to evaluate and retrofit the current structure of residential buildings. With the advent of technology, various steps have been taken by using supports to improve the standards of buildings. The main challenge, however, is strengthening the structure of an existing building without evacuating the residents from the building.

A procedure for evaluating the seismic assessment and strengthening of an existing reinforced concrete (RC) building using shear walls constructed with a mixture of crushed waste tires rubber is proposed to help the elimination of this challenge. This procedure is obtained from a common capacity spectrum methodology with the aim of providing engineers with a technique for estimating the safety margin against structural failure.

1.3 Thesis Objectives

The primary objectives of this thesis focus on providing a method to evaluate and retrofit an existing building. To achieve these objectives, the scope of the thesis covers the following:

- Improving/increasing structural safety and minimizing economic losses.

- Using the real dynamic behavior of the building obtained from forced vibration test results to estimate the properties of building materials and for model calibration.
- Applying an internal strengthening technique to reinforce existing buildings.
- Propose an environmentally friendly, economically viable, fast and reliable method for evaluating and reinforcing buildings.

The aim of this study is to introduce a method for strengthening an RC building through shear walls, using various mixtures of crushed waste tire rubber, and using forced vibration test data to estimate the building material properties without damaging the building.

1.4 Content of Thesis

The primary focus of this thesis is to provide a reliable, fast, economical, and environmentally friendly method for evaluating the seismic properties of existing buildings and constructing shear walls with a mixture of crushed waste tire rubber.

To fully cover the aims of this thesis, five chapters are developed as follows:

Chapter 1 is the introduction: We present a general view of the thesis and the problem statement. Brief explanations of strengthening, the global tire waste problem and the adherence problem of an old structure located in Antakya (Turkey) to seismic safety codes are also presented.

Chapter 2 is the literature review: The literature review chapter covers similar studies that have addressed problems within the same scope. Furthermore, details of different seismic analysis methods are discussed together with their related subtopics.

Chapter 3 is on data collection and methodology: This chapter covers the data collection procedures and required information for the proposed method. The information includes structural conditions, building plans, and material properties. Furthermore, the procedure and stages used in the method are presented in detail. The terminologies are also discussed.

Chapter 4 covers the results and discussion: The results obtained from the structural analysis are discussed in this chapter. The strengthening solutions are also discussed.

Chapter 5 contains the conclusion and recommendations: The summary of the thesis is presented in this chapter. The results are also briefly discussed with the direction for future studies.

Chapter 2

LITERATURE REVIEW

The impact of utilizing recycled materials in today's environment cannot be overstated. Their utility includes the conservation of natural resources by minimizing the amount of required landfill space. Waste rubber is considered to be one of the growing waste products produced by humans. About 10 billion tires are estimated to have been discarded globally in 2005 (Alam et al., 2015). The management of waste-tire rubber is very difficult for municipalities to handle because it is not easily biodegradable, even after long-periods of landfill treatment (Guneyisi et al., 2004). However, recycling waste tire rubber is one alternative. Rubber tires can also be used in civil and non-civil engineering applications, such as in road construction and geotechnical works. Newer technology, such as pyrolysis and devulcanization, has made tires suitable targets for recycling despite their bulk and resilience. Aside from their use as fuel, the main end-use for tires remains ground rubber.

Tire recycling is the process of reusing tires that are not conducive for conventional use for automobile or any other use due to wear and tear or irreparable damage. These tires present a challenging source of waste that requires innovative methods of disposal. Over the past couple of decades, the volume has increased significantly and because tires are highly durable and non-biodegradable, they can consume valuable space in landfills. In 1990, it was estimated that over 1 billion scrap tires were in stockpiles in the United States. From 1994 to 2010, the European Union increased

the amount of tires recycled from 25% of annual discards to nearly 95%, with roughly half of the end-of-life tires used for energy, mostly in cement manufacturing.

Significant advances have been recorded in civil engineering when waste tire is used in structures. Engineers have taken up the task of making waste tire rubber more dependable by crushing them and making use of their mixture with concrete in strengthening existing buildings without totally bringing down the building.

In concrete containing a mixture of waste tire rubber, a 50% decrease in cube and cylinder compressive strength was reported by Topçu (1997). In addition, tensile strength showed a 64% increase with fine rubber particles. About 60% and 80% decreases in cube and cylindrical compressive strength was reported when coarse rubber particles were introduced, while tensile strength also showed a decrease of about 74%. The experimental results are indicative of coarse aggregate having a negative impact on concrete compared to fine rubber aggregate. However, the results obtained by Fattuhi and Clark (1996) present the opposite effect. Their findings concluded that the addition of fine rubber aggregates decreased the compressive strength more significantly than graded coarse aggregate. Their results were in-line with Khaloo et al. (2008), which was also contrary to that of Eldin and Senouci (1993) and Topçu (1997). Studies have shown that Tire Rubber Aggregate Concrete (TRAC) possesses good aesthetics, acceptable workability, and a smaller unit weight than that of ordinary concrete.

2.1 Studies on Mechanical Properties of Crushed Rubber Waste Tires

The research on crumb rubber concrete is motivated by the necessity of recycling waste tire and mitigating the defects in concrete. The dynamic, static, fatigue and other mechanical properties are tested with different volumes of crumb rubber concrete. Topcu (1997) conducted research on the mechanical properties of concrete containing crumb rubber, thus presenting reports on ductility and absorption capacity. Li et al. (2012) investigated the characteristics of two specimens with crumb rubber mixes having the same ratio of replacement but distinct pre-saturated treatment of particles. Their results show that samples with re-saturated rubber have the best mechanical properties, particularly in terms of compressive strength.

The practical application of crumb rubber concrete was presented by Khatib and Bayomy (1999), including the reduction factor effect application. Khatib and Bayomy (1999) inferred that adding rubber particles to concrete leads to an increase in damping ratio and a decrease in the natural frequency of structures. Crumb rubber concrete offers increased dynamic and static properties, which are important in road pavement construction.

A viable option for barriers in concrete high way noise reduction is the crumb rubber blend as identified by Han et al., (2008). It has been applied in composite structures and composite beams, which significantly reduced fatigue behavior. Recycled waste tire rubber is a promising material in the construction industry due to its lightweight, elasticity, energy absorption, sound and heat insulating properties. Eldin and Senouci (1993), Toutanji (1996), Khatib and Bayomy (1999), Siddique and Naik (2004), and

Batayneh et al. (2008) all concluded that over the past two decades, they have performed studies on the availability of using waste tire rubber in concrete mixes.

2.1.1 Tensile Strength

Khatib and Bayomy, (1999) studied and concluded that the tensile strength of rubberized concrete is mostly affected by the size, shape, and texture of the aggregate, and the tensile strength of concrete decreases as the volume of rubber increases, while the toughness and ductility increases. Various failure patterns showed that concrete made with the addition of rubber can have large deformations and still maintain their integrity. The splitting tensile strength of concrete is generally reduced when rubber has been used (Gesoglu, et al., 2014).

2.1.2 Compressive Strength

Khatib and Bayomy, (1999) analyzed the workability of concrete containing crumb rubber as an ideal replacement for sand using different volumes of natural sand replacement from 5% to 100% by volume. Their results show a decrease in workability as the rubber to sand ratio content increases. It was also observed that there was a significant reduction in the compressive strength of concrete whenever tire rubber is used to replace the aggregate in concrete mixtures and when using chipped rubber as a full replacement for the coarse aggregate in a concrete mix. This conforms with the results reported by Eldin and Senouci (1993), Toutanji (1996), and Gesoglu, et al. (2014). Furthermore, there is also a reduction in strength when using crumb rubber as a replacement for sand in the concrete mix.

The compressive strength was significantly decreased when using crumb rubber instead of chipped rubber, and these results conform to the results in Khatib and Bayomy (1999) and that of Siddique and Naik (2004). It is recommended to test

concrete with different percentages of crumb rubber with a silica fume additive to overcome the significant reduction in concrete strength resulting from the replacement of sand by crumb rubber. Figure 2.1 illustrates the compressive strengths from compressive strength and elastic modulus from rubber cement. Group A: in this group, the rubber material was crumb rubber and only replaced the fine aggregate. Eight designated rubber contents in the range of 5–100% by volume of fine aggregate were selected for this group. Group B: tire chips were used to replace the coarse aggregate in this group. Similar to Group A, eight designated rubber contents in the range of 5–100% were used (Khatib and Bayomy, 1999).

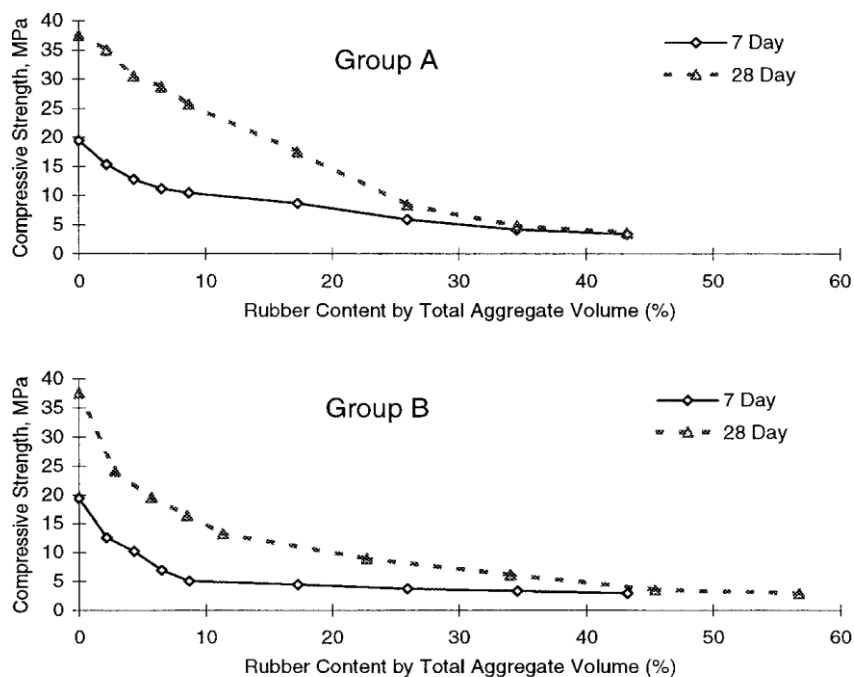


Figure 2.1: Compressive strength (Khatib and Bayomy, 1999).

From the graph given in Figure 2.1, it clearly shows that an increase in the quantity of tire rubber decreases the compressive strength. There was no significant increase in the concrete compressive strength and the concrete density when different

percentages of crumb rubber, as a replacement for sand, was used in the concrete mix (Khatib and Bayomy, 1999).

Rubber can absorb a large amount of plastic energy. Therefore, this concept of rubberized concrete has recently gained interest. Khaloo et al., (2008), observed that increasing the amount of rubber decreases the compressive strength and elastic modulus of concrete while significantly improving its energy-absorption characteristics.

2.1.3 Flexural Failure

Flexural failures are of two types: brittle flexural failure and ductile flexural failure. Brittle flexural failure is characterized by the crushing of concrete before the rebar yields and is very acute because it doesn't provide any warning to the residents of the structure. This kind of failure usually happens to over-reinforced sections. Conversely, ductile flexural failure is characterized by the failure of rebar before the concrete and usually happens with large deformations when the rebar yields. It is a character of under-reinforced sections. Torsional failure is also possible due to shear stress and when the members are located at the sides of the structure,. Rubberized concretes are most commonly applied in non-structural elements, such as floor surfaces, flexible surfaces, and vibrational control applications. They are a perfect candidate for impact-related structures due to their high absorption capabilities. The use of rubberized concrete has not been analyzed in-depth on non-structural applications. The merits of the materials, however, attracted attention mostly in ductility and energy dissipation applications, which are paramount for seismic resistance structures. The replacement of crumb rubber as a coarse and fine aggregate is mostly done at a cost 0.75 times the percentage replacement. This results in a decrease in unit weight, splitting tensile strength, compressive strength, and elastic

modulus. They all have a linear relation to the amount of rubber added (Siddique and Naik, 2004; Khaloo et al., 2008).

2.1.4 Flexural Strength

According to Zborowski et al. (2004), the flexural strength of concrete containing rubber decreases with increases in the content of rubber in the concrete. On the other hand, Kang and Jiang (2008) reported that flexural strength was increased by adding rubber in roller compacted concrete. A flexural strength test was used to determine the flexural strength of concrete. The test was performed on a prism by immersing it underwater. The most important factor in reducing flexural strength, as well as compressive strength, is the lack of good bonding between the rubber particles and cement paste.

The incorporation of crushed rubber tire in concrete exhibits a reduction in compressive and flexural strengths. The reduction in compressive strength is approximately twice the reduction in flexural strength. Zhang, et al., (2015) observed that when the 90 days strength was considered, there was a 28% reduction in the flexural tensile strength of the rubberized specimen (20% crumb rubber) when compared to the control mix specimen. The flexural strength decreases when the amount of rubber was increased from 20 to 30%.

2.1.5 Shear Failure

Shear failure, also known as modulus of rupture, bend strength, or fracture strength, is a material property, defined as the stress in a material just before it yields in a flexure test. The flexural strength represents the highest stress experienced within the material at its moment of rupture. Shear strength is the strength of a material or component against the type of yield or structural failure where the material or component fails in shear. A shear load is a force that tends to produce a sliding

failure on a material along a plane that is parallel to the direction of the force. To put it simply, shear stress is maxed at 45 degrees in the cross-section of a beam, hence a diagonal crack is formed at shear failure, which occurs at the end of the beam where the beam connects to the column. To avoid this type of failure, stirrups are provided in the web of the beam or “shear flexure failure” (see Figure 2.2).

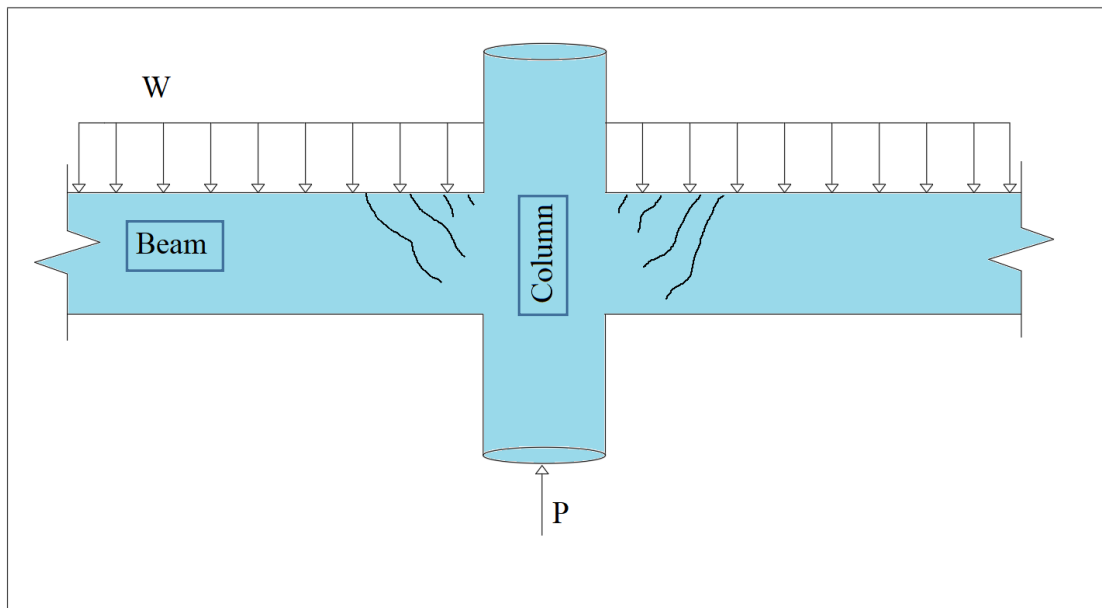


Figure 2.2: Description of Shear failure.

Due to the high local tensile stresses in the web, the “inclined flexural shear cracks” propagate (see Figure 2.2) and reduce the capacity of the different possible shear transfer mechanisms. When the shear transfer capacity between two neighboring portions of the beam becomes too small, a static equilibrium cannot be found. A relative displacement between the two neighboring portions takes place. The shear failure mechanism is characterized by the shear sliding along a crack in the beam without shear reinforcement and the yielding of stirrups in a beam with shear reinforcement.

2.2 Risk of Earthquake

Earthquakes can be defined as the trembling or shaking of the Earth's surface as a result of the sudden release of energy beneath the upper layer of the earth, which creates a seismic wave. The earthquake phenomenon is also known as a tremor or temblor, and in most cases, 'earthquake' is used to describe any seismic event caused by humans as a result of mining, nuclear tests, construction, etc., or natural causes, such as volcanic activity and landslides.

The unchecked growth of the global population led to an upshot in annual earthquake-related losses from 14 billion US\$ in 1985 to more than 140 billion US\$ in 2014. And the average affected population rose from 60 million to over 179 million within the same period.

Earthquakes constitute one-fifth of the annual losses due to natural disasters, with an average death toll of over 25,000 people per year (EM DAT., 2017). An earthquake leads to the occurrence of liquefaction, fire, and tsunamis, which would lead to far higher levels of damage and loss. An assessment of earthquake risk constitutes the first step to making decisions and actions to reduce possible losses (Silva et al., 2014). The process involves developing:

- (a) Sensibility functions establishing the likelihood of loss conditional on the shaking intensity;
- (b) Exposure datasets defining the geographic location and value of the elements exposed to the hazards; and
- (c) Earthquake hazard models depicting the level of ground shaking and its associated frequency across a region.

Risk metrics can assist decision-makers in developing risk reduction measures that can include emergency response plans, the creation of strengthening campaigns, and the development of insurance pools and the enforcement of design codes.

Earthquakes can cause large economic and human losses, and bring about a serious interference in the socio-economic development of a nation (Silva, et al., 2014). Earthquake hazard and risk assessment are fundamental tools for developing risk reduction measures. This process involves developing seismogenic models, selecting ground motion prediction equations, creating exposure models, deriving sets of vulnerability functions, and collecting earthquake catalogues and fault data (Yepes-Estrada, 2017). Combining these components in assessing earthquake hazard and risk requires complex software packages, some of which are currently publicly available. Hazus is one example that has demonstrated how earthquake hazards and risk information can be used to develop risk reduction measures and ultimately alleviate the adverse effects of earthquakes.

2.3 Building Resilience

Risk assessment studies are done to determine how resilient a building can perform in an earthquake-prone environment. The resilience of a building is a combination of its stiffness, strength, and ductility, which suggests the performance of a building during an earthquake. One of these quantities is not sufficient alone: a building that is not ductile may fall or collapse, whereas a ductile building may sway so much that everything within the structure is destroyed. A strong resilient building requires a good combination of these properties, which will result in a satisfactory performance under seismic loading with only a little increase in the construction costs (Kegyes-Brassai and Ray, 2016). The main component of seismic loading is horizontal, while

buildings are designed to withstand a vertical force from gravity, and to a lesser extent, ancillary load and wind applied laterally. The major weaknesses of most structures are lateral. An engineer may use an approach similar to that of evaluating hazard in testing the resilience of a structure. This approach is described below:

1. Perform an analysis adding nonlinear behavior of the soil and foundation as well. Though this method is extremely time-consuming.
2. The pushover analysis is a very common research and design approach. It is done by pushing a structure laterally at a specific location until it collapses. Since the analysis is deflection-controlled and not load-controlled, the structure may soften as it moves. Plastic hinging will take place at different locations and the structure will resist by plastic resilience (Zine et al., 2007).
3. Apply an earthquake history to the base of the structure and determine the nonlinear behavior of the entire structure. Such analysis requires the placement of plastic hinging at important locations.
4. Apply additional lateral static loading to the structure and compute stresses and deformation to see if they are below the required criteria.
5. Perform a model analysis to determine the structure's resonant response and apply a better static coefficient for scaling earthquake load to compute and compare stresses and deflection.
6. Use additional lateral static load values based on earthquake spectra and the fundamental frequency of the building.
7. Apply an earthquake acceleration history to the base of the structure that represents an expected event and compute stresses and deflection.

2.4 Methods for Modelling Seismic Performance

Seismic performance modeling can be categorized into two groups: linear elastic and non-linear methods. The linear method includes model response spectrum analysis and equivalent lateral force analysis, while the nonlinear method includes non-linear time history analysis and pushover analysis. Different computational and experimental methods of evaluating seismic performance were presented by Jeyasehar, et al. (2009).

An estimation of the performance and survivability of structures using the capacity spectrum method, which is an analytical technique, has been used in practice (Deierlein, et al., 1990). The original form of the capacity spectrum method requires the curve of strength capacity to be expressed in the standard spectral acceleration versus period format which is used to estimate the site-specific elastic response seismic demand of an earthquake.

The strength capacity curve was developed based on the pushover analysis by utilizing the code-based inverted triangular loading proportionality or loading distribution to the first mode shape (Army, 1986). The accelerated-displacement response spectrum (ADRS) format was introduced by Mahaney et al. (1993). The method has the advantage of representing the structural capacity and demand in the form of force and displacement on the same plot.

The American Federal Emergency Management Agency (FEMA) and Applied Technology Council (ATC) have recommended methods for obtaining the performance level of structures in seismic action. One of the recommended methods

is the pushover method. The hypothesis behind the pushover method is as follows (Liping et al., 2008):

- The first vibration mode controls the seismic response.
- A shape vector is used to express the structural deformation.
- Floor stiffness is infinite (rigid diaphragm).

A number of studies have utilized the pushover method. Their results show the capability of the pushover method to evaluate structural behavior. Studies like Munshi and Ghosh (1998) used the pushover method to determine structural ductility. Low ductility is a result of weak coupling between shear walls. This has been resolved by increasing the strength of the shear walls. A comparison between the pushover method and the elastic method was made by Krawinkler and Seneviratna (1998). Their results highlighted the ability of the pushover method to identify parameters capable of controlling structural behavior during an earthquake. The study emphasized the effectiveness of the pushover method when structures are vibrated under a fundamental mode. The speed and flexibility of using the pushover method on SAP2000 when analyzing a 3D structure was explained by Ashraf and Stephen (1998).

The dynamic pushover analysis and static pushover analysis were compared by Mwafy and Elnashai (2002) using 12 reinforced concrete buildings that have different characteristics. Their results concluded that static pushover analysis is appropriate for short-period framed structures and low-rise buildings. The potential of utilizing pushover analysis in place of inelastic dynamic time history analysis for seismic design and evaluation was discussed by Elnashai (2001). The study further introduced a novel adaptive pushover method, which considers full multi-model,

spread on inelasticity, spectral amplification, period elongation, and geometric non-linearity within a framework of fiber modeling of materials. A new pushover technique was introduced by Poursha *et al.*, (2009) to consider high-mode effects on structures. The procedure is carried out by testing four special steel moment-resisting frames with different heights and compared with nonlinear analysis. Pushover analysis was also used by Abdi *et al.* (2016) in a sensitivity study to analyze the response modification factor on steel structures in soft-story retrofitted buildings.

In line with the aim of this thesis, which is to develop a fast, inexpensive, and reliable method for evaluating existing RC buildings based on the literature, ATC and FEMA recommendations will be utilized for the nonlinear pushover analysis.

2.5 Strengthening Techniques for RC Buildings

A horizontal load is generated during an earthquake motion, which acts on the structure as a response to the motion created. Figure 2.3 illustrates the horizontal motion during an earthquake and the generated horizontal inertia forces (Kaplan, *et al.*, 2011).

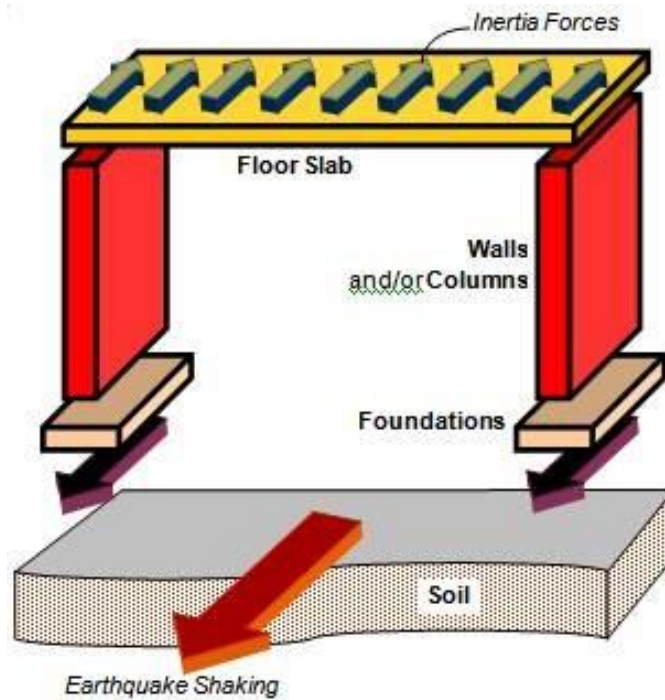


Figure 2.3: Flow of seismic inertia forces through structural components (Kaplan, et al.2011).

The magnitude of displacement is dependent on the stiffness and mass of the building. Minimal horizontal displacement is expected in buildings with high stiffness and low mass. The displacement capacity of every building is peculiar. The primary aim of every strengthening method is to support the building to prevent the displacement from exceeding the capacity (Kaplan et al., 2011). The reinforcement of the buildings is achieved in two ways: either by reducing the expected displacement of the entire structure or by increasing the structural system capacity by imparting ductility to the structure. Multiple techniques exist for improving the strength of RC buildings. They include base strengthening of the building connections, which include reinforced concrete jacketing and steel jacketing, and structural system improvements, such as the infill shear wall and external bracing method.

2.5.1 Strengthening Techniques Base on Strengthening of Building Connection

Reinforced Concrete Jacketing

The main aim of jacketing is to adequately increase the load-carrying capacity of any structural elements against the lateral load it carries. A considerable increase in ductility and stiffness of the section can be achieved depending on the type of jacketing used. Figure 2.4 shows one of the most common techniques which is the Reinforced Concrete Jacketing (RCJ).



Figure 2.4: Reinforced concrete jacketing (source: DEPTA Engineering).

There are basically three methods used in reinforced concrete jacketing. They are: beam jacketing, column jacketing, and beam-column joint jacketing. The main advantages of reinforced concrete jacketing are that it increases the shear and flexural capacity, and is simple to construct. Because of this, it is a widely used technique of strengthening all over the world and several kinds of research work have been done on the utilities and importance of reinforced concrete jacketing. Researchers have concluded that using this method considerably increased the

flexural and shear strength of existing sections. Karayannis and Sirkelis (2008) experimentally investigated and addressed a new type of reinforced concrete jacket for an external beam-column joint damaged by seismic excitations. This experimental procedure was investigated under constantly and continuously increasing cyclic loads, then retrofitted with proposed reinforced concrete jackets and finally retested under the same loading.

The dissipated hysteretic energy area, measured in terms of the area of the full load-deformation envelopes of the original beam-column joint, is compared with the hysteretic energy dissipation of the retrofitted specimens and the comparisons of the seismic performance between the original and retrofitted specimens. The comparison of the seismic performance between the original and the retrofitted specimens shows that all the retrofitted joints using the proposed jacketing with light reinforcement exhibit significantly enhanced behavior with respect to the original specimen. The available structural system geometry and the building mass were not modified, and therefore the dynamic characteristics of the structure remain practically unaffected.

Chalioris and Pourzitidis (2012) applied the self-compacting reinforced concrete technique to a shear damaged reinforced concrete beam. The thickness of the jacket was 25mm and it encased the bottom part of the beam, as well as the vertical side (U-shaped jacket). The steel reinforcement of the jacket consists of small-diameter mild steel longitudinal rebar and U-shaped stirrups. They observed that the load-bearing capacity and structural performance of the jacketed beams were improved with respect to the initially tested specimens. Marlapalle et al. (2014) described the effectiveness of the reinforced concrete jacketing of beams and columns according to (International Standard) IS15988:2013. The authors also described the disadvantages

of the reinforced concrete jacketing technique, such as the available space, which is reduced due to the increase of the section and addition of a large amount of dead mass, and the very slow duration of implementation. Tahsiri et al. (2015) observed from an experimental view that there is an increase in the energy dissipation capacity and ductility; they used ready-mixed concrete for reinforced concrete jacketing to perform an analytical study and compared the results. Minafò (2015) presented an analytical approach to check the strength domain for reinforced concrete jacketed columns and it was based on the stress-block approach. He concluded that the stress-block approach is suitable for the reinforced concrete jacketed column section if all the parameters are well-calibrated. Ahed (2019) experimentally investigated high-performance self-compacting rubberized concrete and evaluated its utility in strengthening RC structures. This study has used high strength concrete to obtain thin jacket thickness, generally between 50 mm and 75 mm, to strengthen the bare columns. He concluded that the performance level of the bare structure was improved from the collapsed state to life safety due to the hinge drifts and damped energy.

Steel Jacketing

External steel elements work to improve column performance by way of increasing the original column confinement and providing additional steel reinforcement that may increase shear strength. However, unlike concrete jacketing, there is no effective increase in section size to directly contribute to the axial capacity increase. From a practical standpoint, steel jacketing causes minimal interruption into the existing space, is relatively simple and quicker to install, and can be low costing.

Plate configuration concerns the most efficient use of the cross-sectional steel area. In this light, Belal et al. (2014) found the ideal configuration to be dependent on the corner plates. When using angles, three batten plates, as compared to six, produced an additional 10% gain in strength and 45% overall. This is advantageous as it reduces the amount of labor. However, using C-shapes resulted in the opposite effect. The fully jacketed section, using thin-plates, produced the lowest strength increase of 19%; although, full jacketing with a suitable thickness can significantly increase strength, ductility, and stiffness (Sezen and Miller 2011). Overall, plate thickness needs to be carefully considered as performance decreases past a certain thickness threshold (He et al. 2106, Sezen and Miller 2011). Similar to Belal et al. (2014), for circular columns, Lai and Ho (2015) found that three steel strips produced strength gains in excess of six strips. Especially in seismic retrofits, ensuring plastic hinging is a top priority. To do so, end stiffeners or thicker batten plates, recommended to be at least 1.5 times the width of the intermediate batten plates, can be used (Xiao and Wu, 2003; Nagaprasad et al., 2009). A recent study related to the steel jacketing technique attempted attaching jackets to the surface of the connection of the structural system as illustrated in Figure 2.5. The length and thickness of the steel required can be calculated using certain parameters, although the steel jacketing technique cannot be modeled in SAP2000 (Choi et al., 2010).



Figure 2.5: Using steel jacketing for connection (Source: RADYAB Engineering Solution).

2.5.2 Strengthening Techniques Based on Improving Structural Systems

Infill Shear Wall

This is a very common strengthening technique. Kahn and Hanson (1979) conducted infill wall-strengthening experiments by testing five one-story one-bay reinforced concrete frames. Two of these specimens were tested as references, one being a bare frame and the other having a monolithically cast shear wall. Three specimens were strengthened with three different infill wall schemes. One wall was cast within an existing frame, a second was precast as a single unit and mechanically connected within the frame, and the third was precast in six individual sections that were mechanically connected to the frame and to each other. All specimens were tested under reversed cyclic loading. According to the test results, the cast-in-place wall showed nearly the same lateral strength as the monolithically cast wall. The infilled wall with six individual precast panels behaved as a series of deep beams, having about one-half the ultimate load capacity of the monolithic specimen.

Phan, Cheok and Todd (1995) analyzed existing experimental research results for seismic strengthening tests in their multi-year research project at the National Institute of Standards and Technology. The objective of this study was to develop guidelines for seismic strengthening techniques by reviewing the experimental observations of 54 lightly reinforced concrete frame tests. The analytical results obtained from the parametric study were used in conjunction with experimental observations extracted from these experimental programs, which were systematically reviewed, and as a result of this study, the following conclusions were suggested as design guidelines for seismic strengthening with cast-in-place or precast panel infills:

- The infill wall thickness, of both cast-in-place and precast infill walls, should be not less than $2/5$ the thickness of the bounding column or the top beam of the frame, whichever is smaller, and should not be greater than the thickness of the top beam.
- Based on experimental observations, the ratio of the total cross-sectional area of the connecting anchors to the area of the infill walls at the wall/frame interface (A_c/A_w) should not be less than 0.8% for a successful connection between the wall and the existing frame.

Numerous researches have shown how this strengthening technique improves the stiffness and lateral load capacity of a building. However, the installation of the shear wall is complex and difficult, as illustrated in Figure 2.6. It is also considered to be expensive because multiple damages are done to the existing structure (Baran, 2005). A study to evaluate the retrofit of an existing RC building without seismic activity

was conducted by Mosalam and Naito (2002). The study showed the structural characteristics before and after masonry infilled frames.



Figure 2.6: Application of infill shear wall in the RC building (Baran, 2005).

Addition of External Bracing Steel in RC Buildings

The addition of external steel bracing to RC structures minimizes seismic action. This strengthening technique is applied to the outside of buildings. The primary advantage of the method is the easy installation across the external facades and axes. In an external bracing system, the steel trusses are introduced to the exterior frames of the building. Bush, Jones, and Jirsa (1991) conducted cyclic loading tests on 2-scaled 3D models of a number of structures retrofitted using external bracing. The main frame included deep, stiff spandrel beams and short, flexible columns that were susceptible to shear failure under lateral loads. A steel X-bracing system attached to the exterior of the frame using epoxy grouted dowels was used to strengthen the existing frame. The frame model consisting of two bays and three levels was subjected to a statically-applied cyclic lateral load. While evaluating the prototype

under lateral loading, the nominal column shear capacity would be exceeded when only 40% of the column flexural capacity and 30% of the beam flexural capacity were reached. Bracing system elements attached to the side faces of the concrete columns also significantly increased the column shear capacities. The lateral capacity of the strengthened frame was governed by brace buckling, eventual connection failures, and column shear failures. Badoux and Jirsa (1990) numerically investigated the behavior of RC frames retrofitted with external bracing. They concluded that the lateral resistance of the existing frame structures is inadequate for two reasons. First, the perimeter frames, which feature weak short columns, are likely to fail in an undesirable mode. Secondly, code provisions may have been upgraded several times since construction, so that current seismic design loads are more than the original values. Based on these conclusions, Badoux and Jirsa (1990) recommend that the designer must consider the failure mechanism of the original frame under lateral deformations. The bracing system can improve the frame strength and stiffness, but cannot change the frame mode of failure. The weak column-strong beam frame leads to an unwanted mode of failure so this of type frame should be transferred into a strong column-weak beam frame. This can be achieved by strengthening the columns or by weakening the beams.

Figure 2.7 illustrates the utilization of the buttress-type steel shear wall on external building facades. Alhashimi (2018) studied an existing RC building to evaluate and retrofit it using bracing steel. The study showed two types of braced steel frames to evaluate structural performance before and after strengthening. The first type is shaped like an inverted V and the second one is shaped like an X. He concluded that the demand curve showed a significant improvement.

A comparison between the bracing connected to the RC frame method and infill masonry walls method was made by Prakash and Thakkar (2003) using a 14-story RC building located in seismic zone IV. Their results indicate that the cross patterns of steel bracing have a better seismic performance than the rest.



Figure 2.7: External steel bracing frame out of a structure (Prakash and Thakkar, 2003).

2.6 Past Studies on Pushover Analysis

Most of the simplified nonlinear analysis procedures utilized for seismic performance evaluation make use of pushover analysis and/or an equivalent SDOF representation of the actual structure. However, pushover analysis involves certain approximations that should be identified for the reliability and the accuracy of the procedure. For this purpose, researchers investigated various aspects of pushover analysis to identify the limitations and weaknesses of the procedure and proposed improved pushover procedures that consider the effects of lateral load patterns, higher modes, failure mechanisms, etc.

Krawinkler and Seneviratna (1998) conducted a detailed study that discusses the advantages, disadvantages, and applicability of pushover analysis by considering various aspects of the procedure. The basic concepts and main assumptions on which the pushover analysis is based, target displacement estimation of the MDOF structure through the equivalent SDOF domain and the applied modification factors, the importance of lateral load pattern on pushover predictions, conditions under which pushover predictions are adequate or not, and the information obtained from pushover analysis were identified. The accuracy of pushover predictions were evaluated on a 4-story steel frame damaged in the 1994 Northridge earthquake. The frame was subjected to nine ground motion records. Local and global seismic demands were calculated from the pushover analysis results at the target displacement associated with the individual records. The comparison of pushover and nonlinear dynamic analysis results showed that pushover analysis provides good predictions of seismic demands for low-rise structures having a uniform distribution of inelastic behavior over the height. It was also recommended to implement pushover analysis with caution and judgment considering its many limitations since the method is approximate in nature and contains many unresolved issues that need to be investigated.

Chapter 3

METHODOLOGY AND DATA COLLECTION

3.1 Introduction

The procedure that was used to conduct this study is outlined in this chapter and involved numerous steps, including: data collection, estimation of the building's mechanical material properties, seismic performance analysis, and strengthening with shear walls constructed using crushed waste tires rubber. Moreover, it also contains some detailed explanations about the methods and major terminologies.

3.2 Research Methodology

This study includes three stages. First, data regarding the structural plans, building frame, and material properties were collected. By coupling the forced vibration data of the structure, the modulus of elasticity is estimated with the analytical modal behavior from SAP2000. Second, a simulation model of the building was created so that an evaluation of the behavior of various lateral loads resistance on the existing RC frame can be conducted. ATC 40 pushover methodology on SAP2000 was used to conduct this analysis and its outputs include performance levels, the behavior of plastic hinges, and the location of possible weak elements on the structure of the existing building. Third, the seismic strengthening design of the building was obtained and evaluated using the ATC 40 pushover analysis methodology. The strength of the building structure is increased by using shear walls that are infilled in some of the RC frames of the building. The enhanced performance of the existing building was studied in detail in terms of demand curves, hinge formation, moment-

rotation, capacity spectrum, and the performance level of the building. The procedure of all three stages is shown in Figure 3.1.

The major purpose of this procedure is to update the current existing building to meet the current TEC 2007.

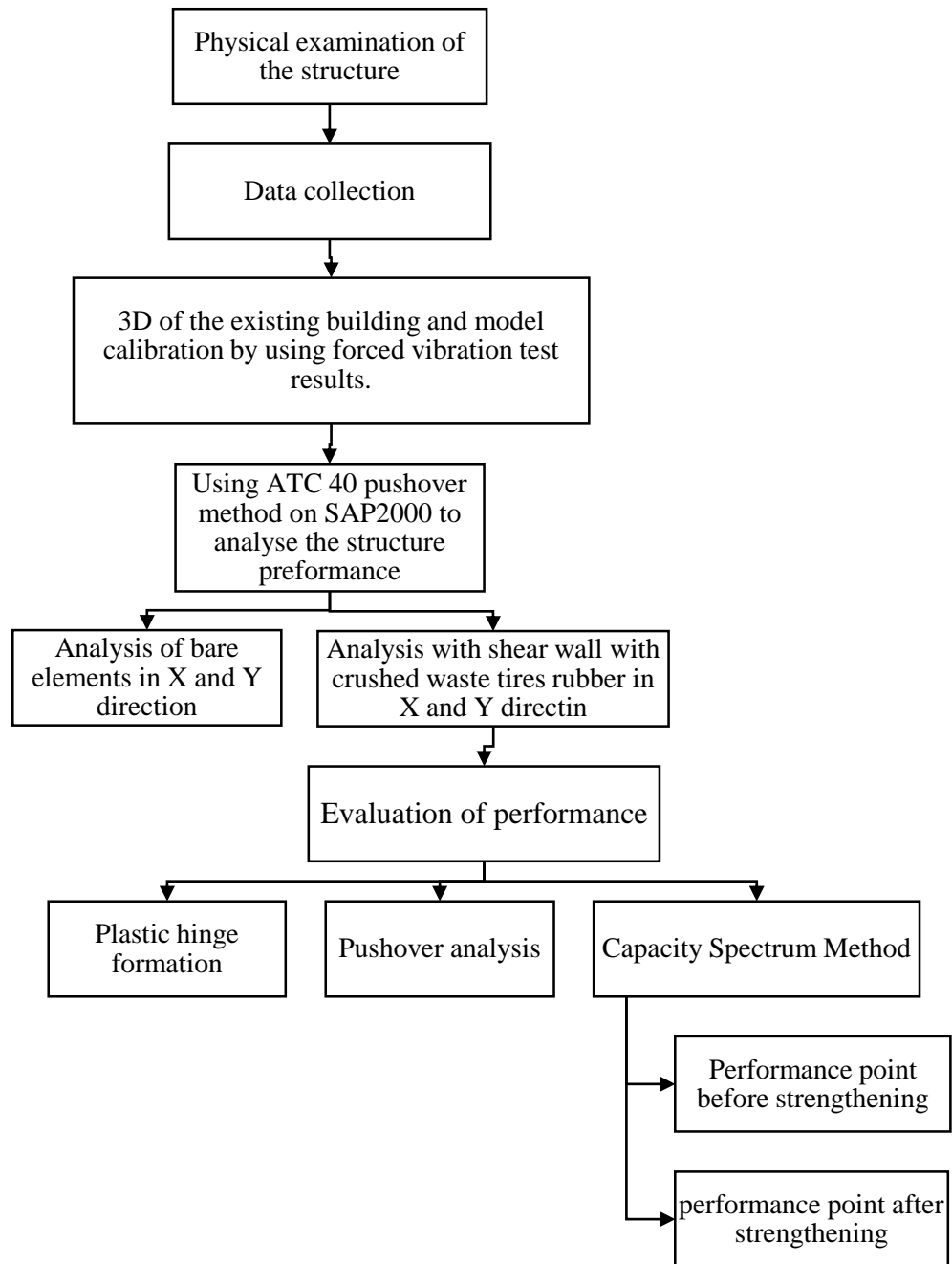


Figure 3.1: Analysis of the existing building.

3.3 Data Collection

3.3.1 Information About the Building Under Study

This study investigates the strengthening and seismic evaluation of an existing building. The building is a 5-story apartment located in the suburbs of Antakya, Turkey, which was built in 1988. It is located at $36^{\circ}12'17.78''N$ $36^{\circ} 8'39.67''E$ according to Google Earth Map 2019, shown in Figure 3.2. The city is in seismic zone I.

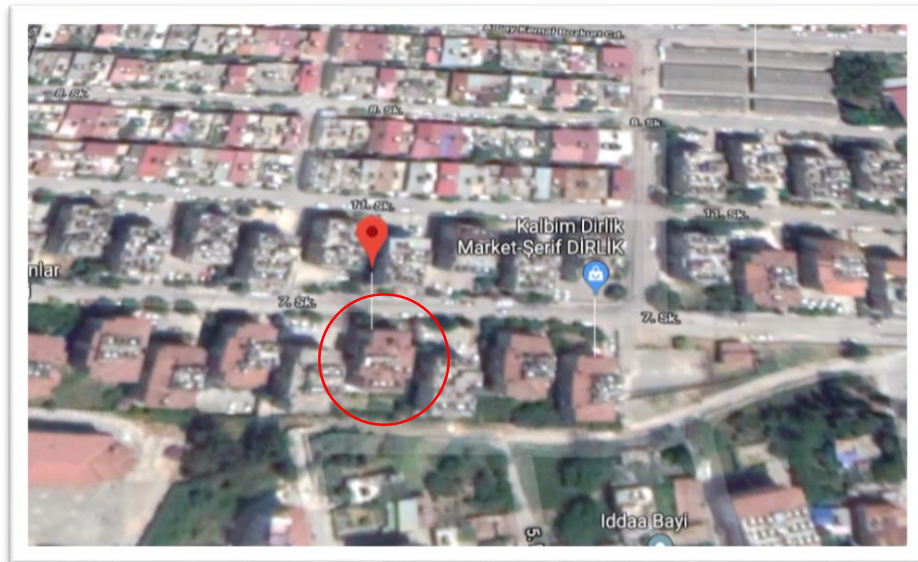


Figure 3.2: Location of studied apartment in Antakya, Turkey.

3.3.2 Building Details

The apartment is a five-story RC building. The building dimensions are 23 m length, 14.4 m width and 3 m height for each floor (Figure 3.3). The whole design of the building, floor designs, and section dimensions are provided in Appendix A.



Figure 3.3: Studied apartment view in Antakya, Turkey.

The main dimensions collected about the building are as follows:

1. Building plans and dimensions of span, height, length, and width, which have been provided and shown in Figures A1 and A2 in the Appendix.
2. Slab design of reinforcements for the ground and normal floors are shown on plan in Figures A3 and A4 in the Appendix.
3. The column designs of reinforcements for each floor design are shown on plans in Figures A5 to A8 in the Appendix.
4. The beam designs of reinforcements for normal floors design are shown on plans in Figures A9 to A17 in the Appendix.
5. Marking short columns and other comparative issues.

3.3.3 Material Properties of the Building

The methods that have been used to determine the modulus of elasticity of the existing building are as follows: tension (or compression) test on the core specimen, bending test, some non-destructive-method and forced vibration tests on the structure.

The tension and/or completion bending test are based on the principle of Hooke's law and they are known as static methods.

In this study, the natural vibration frequency of the structure is determined based on the forced vibration test results provided from study of Genes et al., (2011). The dominant vibration period and the mode shapes of the building were determined by using a vibration generator and some sensors on the existing building. Applying the modal analysis of a building in SAP2000 can define the theoretical dynamic vibration behavior of the building, which compared with real dynamic vibration parameters of the structure by changing the modulus of elasticity or strength of the concrete. The modulus of elasticity or strength can be changed in the model until the theoretical vibration period becomes equal or close to the real one obtained from the forced vibration test (Genes et al., 2011). This method is called model calibration.

According to vibration tests conducted by Genes et al. (2011), at a given frequency both the applied load and the response are theoretically sinusoidal with the same frequency. The treatment of the recorded data can be carried out by eliminating some noises from electrical, mechanical and ambient sources. The vibration generator used in this test has a working frequency of 0.5 to 15 Hz and is capable of producing a sinusoidal force. The shaker is shown in Figure 3.4.



Figure 3.4: The shaker.

As a data acquisition system, only six velocity meters (each one has three channels: x , y , and z) could be connected to the Network Control Centre (NCC) used; the locations of the sensors were selected in order to determine the first dominant lateral vibration periods in both directions (x and y) and the torsional period of the building (Figure 3.5). The arrangement of the sensors is performed as follows: two sensors are located on the top floor and two other sensors are located on the third floor of the building but at opposite corners. The fifth sensor is located at the corner of the ground floor. In addition, the sixth sensor is located at the entrance of the building. Since all the sensors have three channels, there was no need to change the direction of the sensors during the tests. The data processing was performed by using View 2002 software performed by Syscom Instruments and developed by Ziegler Consultants in Zurich, Switzerland. Figure 3.6 illustrates the locations of the accelerometer sensors and vibration generator in the building.

The shaker has two arms where each arm can be loaded with sets of masses weighing 660 grams. To determine the dynamic properties of the building, records are

collected from shaking the building in x- and y-direction, and were used to determine the dynamic properties of the building by averaging the records from the velocity meter's channels oriented in the same direction, and the torsion properties were identified based on the difference in these records. The records are based on the resulting displacement-time responses at different stories and their phase difference, and mode shapes could be collected from the ratios of the amplitudes. As resonant frequencies were known at this stage, only responses at these frequencies were actually needed.



Figure 3.5: Sensors by syscom.

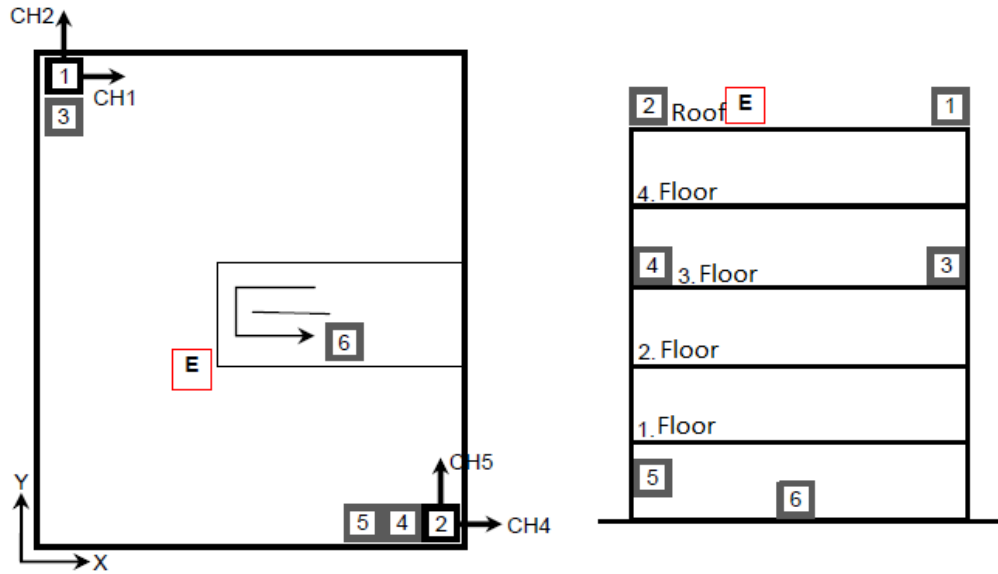


Figure 3.6: Layout of the building accelerometer sensors and vibration generator.

3.3.4 Modeling of Infill Walls

In many design regulations and structure analysis programs today, brick infill walls are only considered as constant load but do not contribute to the lateral stiffness of the building. This assumption is acceptable. However, infill walls constructed between the columns partially restrict horizontal displacements and thus affect the building's seismic behavior, such as modal periods, mode shapes and horizontal load-bearing capacity.

Due to the complexity of the effect of brick walls on multi-story buildings, it cannot be said that a reliable modeling method has been developed. Nevertheless, the stresses between the frame and the filling wall, rather than dispersed, were found to be concentrated in the pressure region at the endpoints (Figure 3.7). It is also a practical method that forms the basis for most of today's studies. An Equivalent Virtual Pressure Bars Method has been proposed by Mainstone (1971)

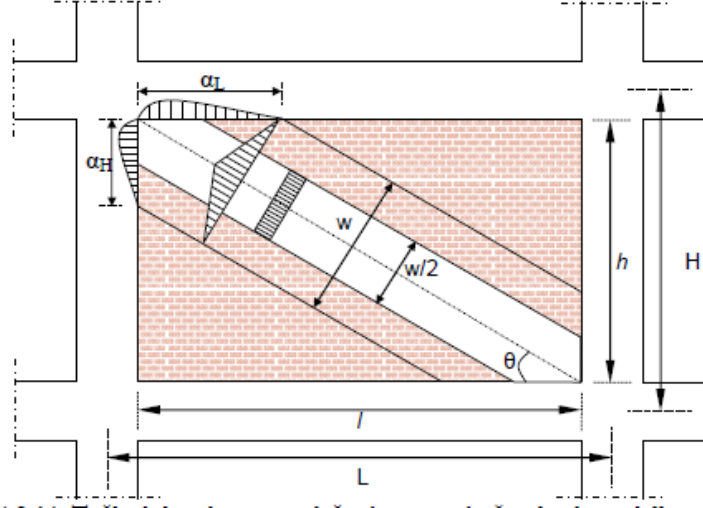


Figure 3.7: Modeling of brick infill wall as equivalent pressure strut.

$$W_{wall} = 0.175 * (\lambda * H)^{-0.4} * \sqrt{h^2 + l^2} \quad (3.1)$$

$$\lambda = \sqrt[4]{\frac{E_{wall} * t_{wall} * \sin 2\theta}{4 * E_{frame} * I_{column} * h}} \quad (3.2)$$

$$\theta = \tan^{-1} \left(\frac{h}{l} \right) \quad (3.3)$$

Here, W_{wall} represents the width of the wall equivalent virtual pressure bar, λ the equivalent pressure bar coefficient, H the length of the column, L the opening of the frame, h the length of the wall, l the width of the wall, E_{wall} the modulus of elasticity of the wall, E_{frame} the elasticity module of the wall frame material, t_{wall} the thickness of the wall, I_{column} the moment of inertia of the small cross-section of the columns in the wall direction, and θ is the angle that the equivalent pressure rod makes with the horizontal.

3.3.5 Modeling the Building and Model Calibration the Building

The building was modeled using SAP2000. The infill walls are considered a compression strut in the model. By applying the aforementioned method, the modulus of elasticity of the building is obtained as 30000 MPa. The compression strength of the concrete can be obtained according to the Turkish Standard (TS500,2000) using $E_c = 3250\sqrt{f'_c} + 14000$ (MPa). Where, f'_c is the cylinder characteristic strength of the concrete. The detailed analysis and work is presented in Chapter 4.3. The summary of the study is given in Table 3.1.

Table 3.1: Vibration frequencies and periods.

Building		X-Direction			Y-Direction		
		Sensor 1 (Hz)	Sensor 2 (Hz)	Period	Sensor 1 (Hz)	Sensor 2 (Hz)	Period
Forced Vibration	Mode I	4.2	4.2	0.24	3.8	3.4	0.28
	Mode II	-	-	-	4.8	4.6	0.21
Analytical Analysis (without shear walls)	Mode I			0.48			
	Mode II						0.47
Analytical Analysis (with shear Walls)	Mode I			0.35			
	Mode II						0.32

The first row of Table 3.1 shows the result of the forced vibration test as frequencies and periods. The modal analysis of the building model in SAP2000 records that the period of mode I is 0.48, and mode II is 0.47 for without brick walls consideration. Moreover, the partition walls added to the model as compression strut element to

reflect the stiffness contribution of real building. The modal analysis of the building model with shear walls is given in the third row of Table 3.1.

3.4 Seismic Assessment of the Building

The seismic assessment of a building can be done by pushover analysis. In pushover analysis, the force from the earthquake is simulated as a lateral force acting on the mass center of each floor of the building following different load patterns (i.e. uniform, triangular, and modal). The lateral force is increased gradually until the target displacement is reached. The target displacement depends on the design of the earthquake behavior and building capacity while the amount of damage relies on the magnitude of ground shaking.

Relevant terms techniques are given in ATC 40 (1996) which is provided in SAP2000.

3.4.1 The Capacity Spectrum and Demand Spectrum

The capacity spectrum method (CSM) is a nonlinear static analysis method that graphically compares both the overall lateral resistance capacity curve to an earthquake demand curve. The lateral resistance capacity curve can be shown using a force-displacement curve from a pushover analysis. On the other hand, earthquake demand is represented by the earthquake response spectrum curve. In addition, the acceleration and displacement spectral values are generated from the corresponding response spectrum for a certain damping ratio. The Acceleration versus Displacement Response Spectrum (ADRS) graph shows all the curves on the same graph as shown in Figure 3.8. The equivalent damping and natural period of a building increases by increasing the nonlinear deformation. It is clear that the instantaneous demand point moves to a different response spectrum by changing the

damping. The demand spectrum line is the track of the demand points in the ADRS plot.

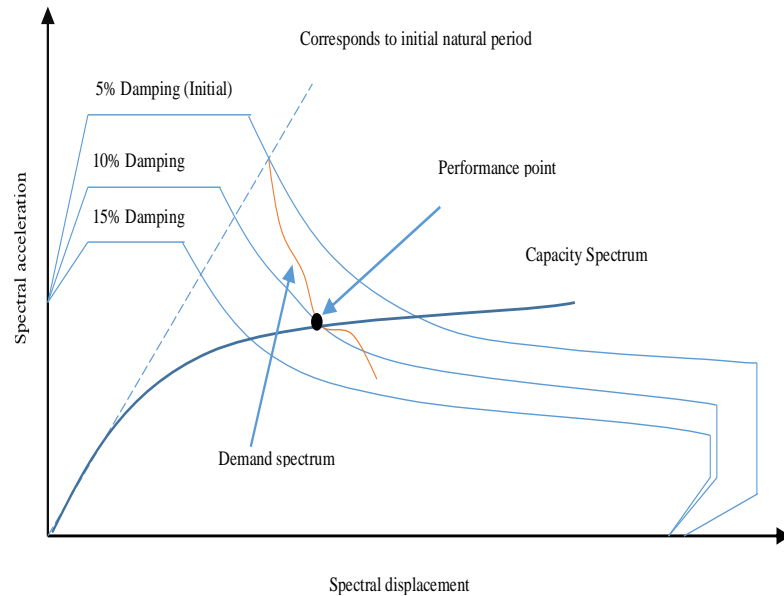


Figure 3.8: Demand and capacity spectrum (Vijayakumar et al., 2012).

Displacement-Based Analysis

Displacement-based analysis is a procedure that estimates the expected deformation, lateral displacements, and inelasticity of a structure according to an earthquake's ground motion. Some demand considering, in displacement-based design methods, the first mode of vibration as the start point. The distribution and demand of both moments and shears along the vertical elements have significant effects. Nonlinear static pushover analysis is the best example of this.

Elastic Response Spectrum

A 5% damped response spectrum for every signal seismic risk level of attention represents the maximum response of the building in terms of spectral acceleration (S_a) at any period throughout a shaking as a function of the period of vibration T .

Performance Point

The performance point is the point where the capacity spectrum curve crosses the demand spectrum, as shown in Figure 3.8. If the performance point exists and the damage state at this point is satisfactory, then the building is considered to be acceptable for the design of lateral forces. To meet performance standards, the structure should be designed to tolerate this degree of load.

3.4.2 Displacement Coefficient Methodology (FEMA 356)

This is the process of calculating a performance point by using the elastic spectrum from the capacity curve (FEMA 356). The top point of a building is targeted to a displacement (δ_t), which is consistent with the performance point that has been calculated by using:

$$\delta_t = C_0 C_1 C_2 C_3 S_a \frac{T_e^2}{4\pi^2} g \quad (3.4)$$

Where: C_0 is the coefficient correlating to the displacement; C_1 is the modification factor to relate expected maximum inelastic displacements to displacements; C_2 is the modification factor to represent the effect of pinched hysteretic shape, stiffness degradation and strength deterioration on maximum displacement response; C_3 is the modification factor to represent increased displacements due to dynamic P- Δ effects; S_a is the response spectrum acceleration at the effective fundamental period and damping ratio of the building in the direction under consideration; T_e is the effective fundamental period of the building in the direction under consideration; and g is the gravitational acceleration.

In addition, the target shear (V_t) is calculated from FEMA 356 using the relation given below (EQ 3-10 in FEMA 356)

$$V_t = C_1 C_2 C_3 C_m S_a W \quad (3.5)$$

Where C_m is the effective mass factor to take in the account the higher mode mass participation effects obtained from Table 3-1 in FEMA 356 and W is the total building weight.

3.4.3 Performance Levels of Building

FEMA 356 outlines the limitations on acceptable damages that a building can have in case of an earthquake. The limiting condition considers the building's physical damage, life-safety hazard because of the damage, and the post-earthquake serviceability of the building.

Yield Point (B)

Yield point is the ultimate capacity that a structure can reach. It is also the end of linear elastic force-deformation relationship where the effectiveness of stiffness begins to decrease.

Immediate Occupancy (IO)

The damages caused by the earthquake are very low. Horizontal and vertical load-resisting systems maintain most of their original characteristics. The risk of great harm from structural damage is irrelevant.

Life Safety (LS)

The vital structural elements are intact and remain, while minor damage during the earthquake might happen. The risk is not life-threatening, however, rapid repairs to the structure are expected before re-occupation. Sometimes repairs are not economically viable.

Collapse Prevention Level (CP)

This level of a building performance includes the collapse of structural components, also excludes non-structural weakness except parapet wall attachments.

Primary Elements and Secondary Elements (E)

Primary elements are those required to withstand horizontal forces after many inelastic responses to earthquake movements. Secondary elements are those required to sustain gravity forces and some horizontal forces.

The three structure performance levels based on TEC 2007 are as follows: immediate occupancy (IO), life safety (LS), and collapse prevention (CP). The performance levels are defined based on the damage that they cause to the structure as follows:

- Immediate occupancy (IO): the maximum allowed damage in each story is 10% of the beam sections. The beam damage must be between the IO and LS limits. However, damage to the rest of the structural members should be less than IO.
- Life safety (LS): the limit is 30% of the beams can be between LS and CP, except for the secondary members. However, the acceptable damage to columns must be between LS and CP for each story. The effect of shear forces should not stay any lower than 20% of the whole shear forces. For members between LS and CP levels, the total shear forces of columns on the top story can be a maximum of 40% of the related story's shear forces of all columns. The rest of the structural members should be lower than LS limits. For brittle members, the member can be assumed to be in the LS limit.

- Collapse prevention (CP): a maximum of 20% of the beams must be beyond the CP limit except the secondary members. The shear stress should be less than 30% of all column's shear capacity when the column passes the IO limit.

3.4.4 Nonlinear Plastic Hinge Properties

This acquires the deformation curve of beam sections, column sections, and masonry by use of FEMA 356. The curve of shear force-deformation is taken from details of reinforcement for components of the building. By using the section designer in the SAP2000 model, all non-linear properties for columns and beams are evaluated. The shear hinge (V2) and the flexural hinge (M3) are applied to two ends of the beam. The hinge interaction of (P-M2-M3) is applied to upper and lower ends of the columns.

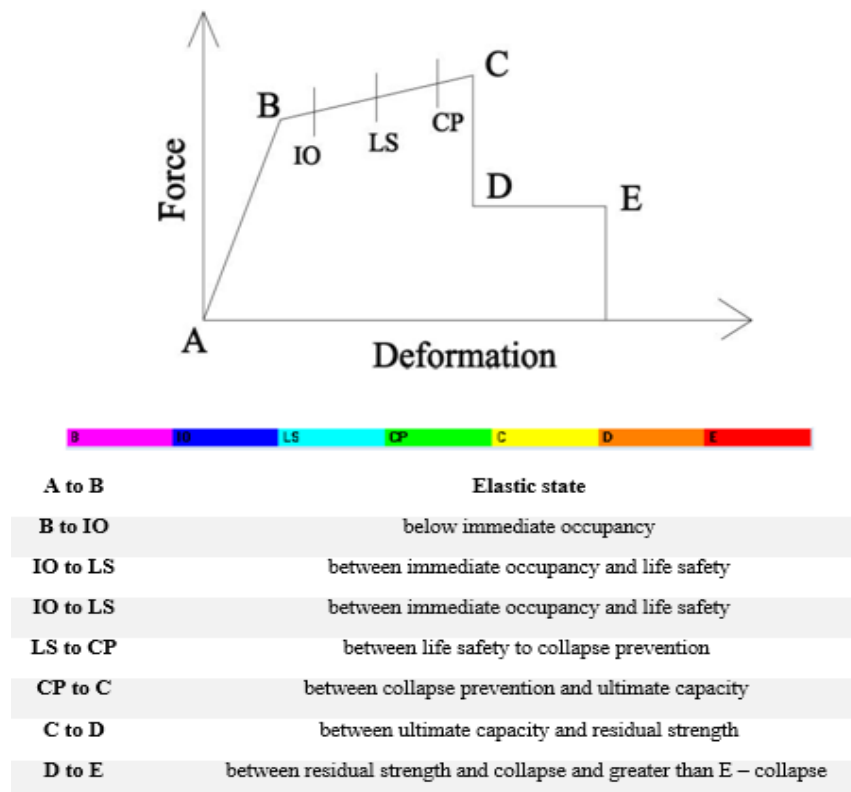


Figure 3.9: Different stages and definitions of plastic hinges (Vijayakumar, et al. 2012).

The axial hinge (P) is applied to the compression strut elements. Subsequently, the pushover analysis has been controlled for the roof structures. As a result of the position of hinges, several steps can be performed for the hinges stages as shown in Figure 3.9.

3.4.5 Pushover Analysis Applications in SAP2000

Properties and parameters must be collected in order to apply the building model in SAP2000. As mentioned before, the modulus of elasticity of the concrete is determined during model calibration. The existing compressive strength of concrete is determined by the formula provided in TS500 and the existing steel reinforcement tensile strength is determined from the specified steel type in project of the building. The other seismic parameters, such as seismic zone factors, building importance factor, live load participation factor and soil condition are collected as shown in Table 3.2 (Özşahin and Değerliyurt 2013).

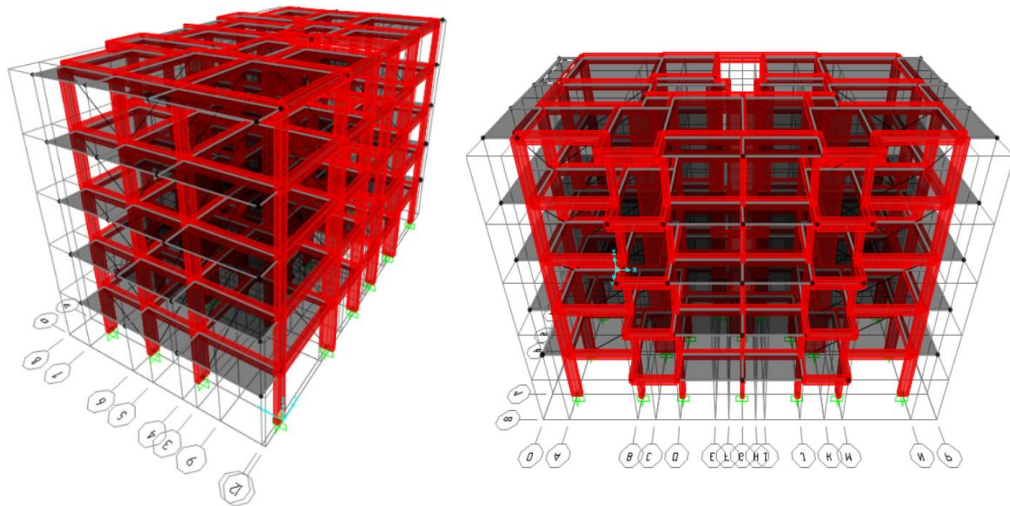


Figure 3.10: Three dimensional model of the building.

The basic 3D model of the building was created from the original plan as shown in Figure 3.10. The plans of the building are given in the Appendix.

Table 3.2: Existing properties and code parameters of the building.

Existing Building Properties	
Knowledge level	Moderate
Modulus of Elasticity	30000 MPa
Knowledge level factor	0.9
Existing concrete compressive strength	25 MPa
Existing steel reinforcement tensile strength	220 MPa
Earthquake Code Parameters	
Seismic Zone	1
Seismic Zone Factor (A_0)	0.1
Building Importance Factor (I)	1.0
Soil Class	Z4
Live Load Participation Factor	0.3

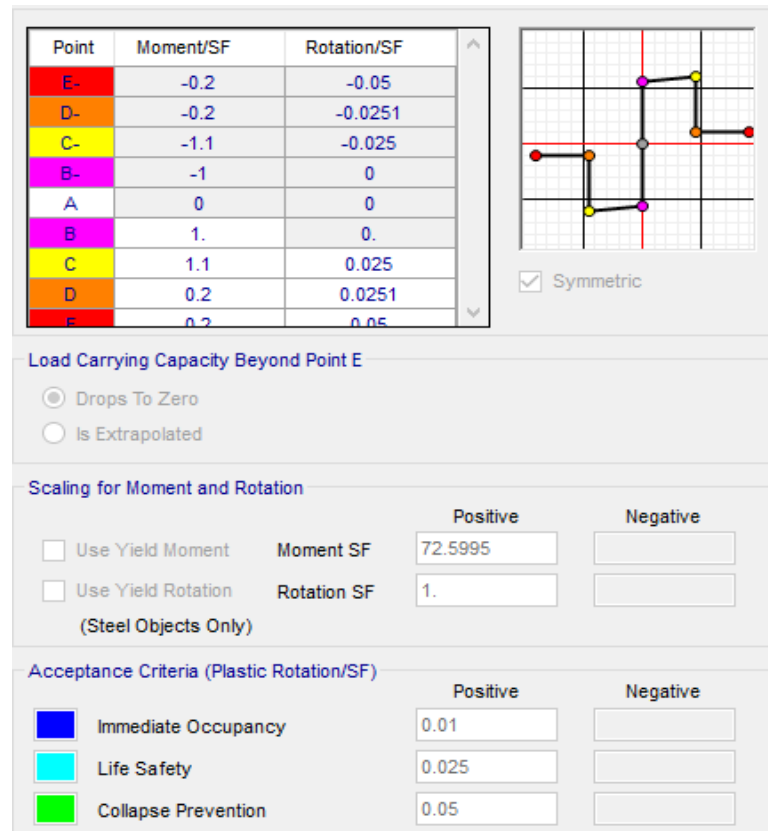


Figure 3.11: Default hinge properties of the frame.

- The software offers many hinge properties that are undertaken for RC concrete elements in order to define their behaviour during the pushover analysis (ATC-40) as shown in Figure 3.11.
- The plastic hinges on the model into SAP2000 were positioned by selecting the frame members, and then assigning hinge properties to them at hinge positions.
- The pushover cases were defined in SAP2000, where more than one pushover load case can be run in the same analysis. Moreover, a pushover load case can be started from the final conditions of another pushover load case, which was before run in the same analysis. Typically, the first pushover load case is used to put on a gravity load, and then following a lateral pushover load, cases are quantified to start from the final conditions of the gravity pushover. Pushover load cases can be force measured (i.e. pushed to a certain defined force level) under control of the displacement (i.e. pushed to a specified displacement).
- The pushover curve is shown in the system when running the analysis. A table, which gives the coordination of each step of the pushover, summarizes the number of hinges in each state as defined between IO and LS or between D and E.
- Next, the capacity spectrum curve is displayed. The performance point for a given set of values is defined by the intersection of the capacity curve and the single-demand spectrum curve.
- The pushover displaced shape and sequence of hinge formation are reviewed on a step-by-step basis. Hinges appear when they yield and they are color-coded based on their state.

3.5 Performance-Based Earthquake Engineering

Performance-based earthquake engineering practice arose from the realization that the problems in the seismic behavior of structures had to do with the approach of designing them explicitly for life safety, thus not attempting to reduce damage in a structure and minimize economic losses.

The performance-based methodology necessitates the estimation of two quantities for assessment and design purposes. These are seismic capacity and seismic demand. Seismic capacity signifies the ability of the building to resist the seismic effects. Seismic demand is a description of the earthquake effects on the building. The performance is evaluated in a manner such that the capacity is greater than the demand (ATC-40, 1996). These quantities can be determined by performing either inelastic time-history analyses or nonlinear static ‘pushover’ analyses.

3.5.1 Nonlinear Static Analysis Procedure (Pushover Analysis)

The nonlinear static analysis (NSP) procedure is normally called the Pushover Analysis (POA). POA is a technique in which a computer model of a structure is subjected to a predetermined lateral load pattern, which approximately represents the relative inertia forces generated at locations of substantial mass. The intensity of the load is increased, i.e. the structure is ‘pushed’, and the sequence of cracks, yielding plastic hinge formations, and the load at which failure of the various structural components occurs is recorded as a function of the increasing lateral load. This incremental process continues until a predetermined displacement limit.

3.5.2 Capacity Spectrum Method (CSM), (ATC 40)

The Capacity Spectrum Method (CSM) is a rapid seismic assessment tool for buildings. Subsequently, the method was accepted as a seismic design tool. The steps in the method are as follows:

3.5.3 Nonlinear Static Pushover Analysis of the MDOF Model

In order to perform a pushover analysis for an MDOF system, a pattern of increasing lateral forces needs to be applied to the mass points of the system. The purpose of this is to represent all forces which are produced when the system is subjected to earthquake excitation. By incrementally applying this pattern up to and into the inelastic stage, progressive yielding of the structural elements can be monitored. During the inelastic stage, the system will experience a loss of stiffness and a change in its vibration period. This can be seen in the force-deformation relationship of the system. A vertical distribution of the lateral loading to be applied to the structure is assumed based on the fundamental mode of vibration. A nonlinear static analysis is then carried out to give a Base Shear – Roof Displacement Curve, or in another words the Capacity Curve.

3.5.4 Definition of Inelastic Equivalent SDOF System

The capacity curve is then approximated as a bilinear relationship with the choice of a global yield point (V_y, u_y) of the structural system and a final displacement (V_{pi}, u_{pi}). The yield point (V_y, u_y) is defined such that the area A_1 in Figure 3.12 is approximately equal to the area A_2 in order to ensure that there is an equal amount of energy associated with each curve.

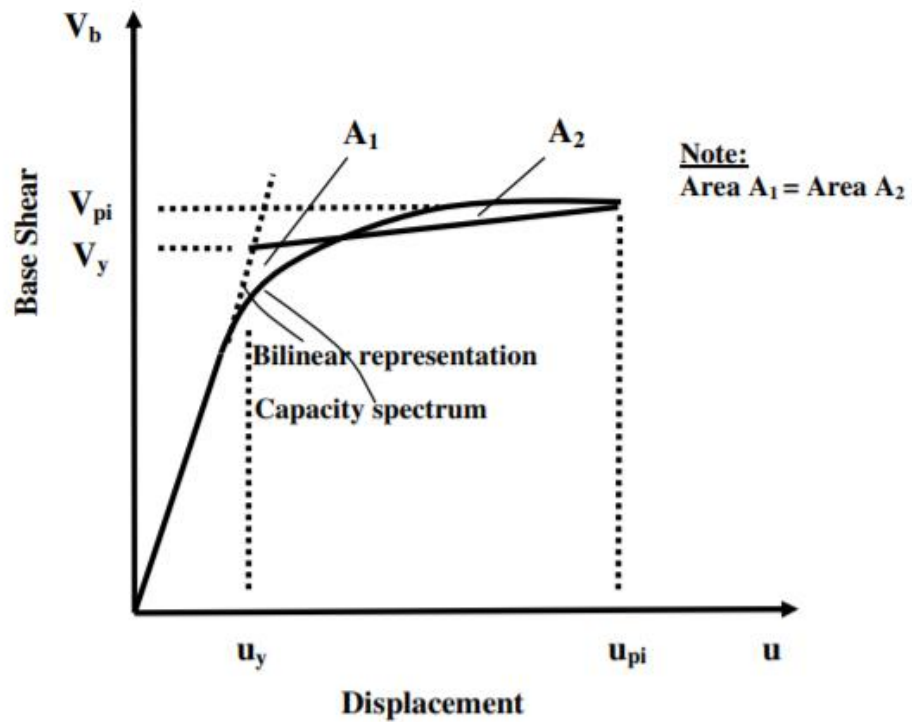


Figure 3.12: Bilinear approximation of the capacity curve

3.5.5 Conversion of Capacity Curve to Capacity Spectrum

The Capacity Curve is then converted to a Capacity Spectrum relationship using the following equations:

$$S_a = \frac{V_b}{\alpha_m \cdot M} \quad (3.6)$$

$$S_d = \frac{u}{PF_1 \phi_{ij}} \quad (3.7)$$

Where M is the total mass of the building, ϕ_{ij} is the modal amplitude at story level 'i' for mode j , PF_1 is a participation factor, and α_m is the modal mass coefficient which is given as:

$$PF_1 = \frac{\{\Phi\}^T [M] \{1\}}{\{\Phi\}^T [M] \{\Phi\}} \quad (3.8)$$

$$\alpha_m = \frac{\left[\sum_{j=1}^n m_i \phi_{ij} \right]^2}{\sum_{i=1}^n m_i \sum_{j=1}^n m_i \phi_{ij}^2} \quad (3.9)$$

3.5.6 Superposition of the Capacity Spectrum on the Elastic Damped Demand Spectrum

Once the capacity spectrum and the 5% damped elastic demand spectrum are plotted together in the Acceleration-Displacement Response Spectrum (ADRS) format, (Figure 3.13), which is an initial estimate of the performance point (a_{pi} , d_{pi}) using the equal displacement rule, can be obtained by extending the linear part of the capacity spectrum until it intersects the 5% damped demand spectrum. Alternatively, the performance point can be assumed to be the endpoint of the capacity spectrum or might be another point chosen on the basis of engineering judgment, as the ATC-40 has suggested.

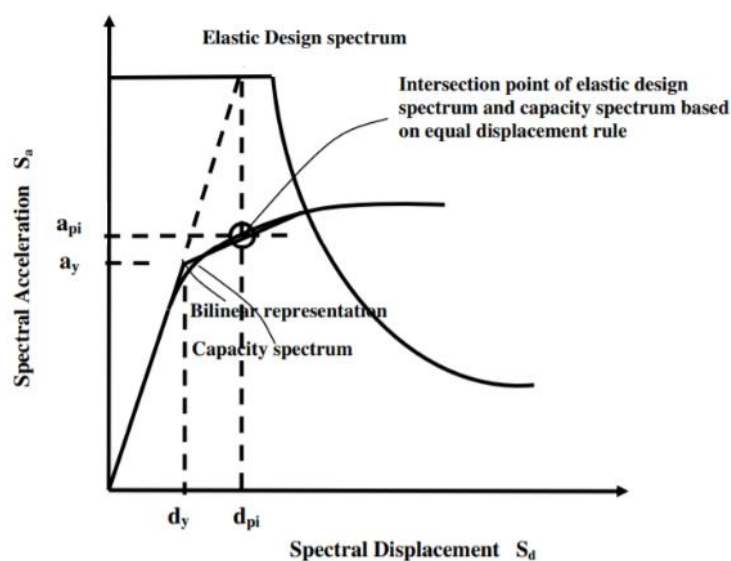


Figure 3.13: Initial estimation of performance point using the Equal Displacement rule

3.5.7 Equivalent Viscous Damping

When structures enter the nonlinear stage during a seismic event, they are subjected to damping, which is assumed to be a combination of viscous damping and hysteretic damping. Viscous damping is generally accepted as an inherent property of structures. Hysteretic damping is the damping associated with the area inside the force-deformation relationship of the structure and is represented by an equivalent viscous damping.

3.5.8 Performance Point of Equivalent SDOF System

The demand spectrum should then be checked if it intersects the capacity spectrum at or close enough to the estimate of the performance point (Figure 3.14). If the demand spectrum intersects the capacity spectrum within an acceptable tolerance then the estimate is accepted. Otherwise, the performance point is re-estimated and the procedure is repeated from the step of superimposing the capacity spectrum on the ADRS spectrum.

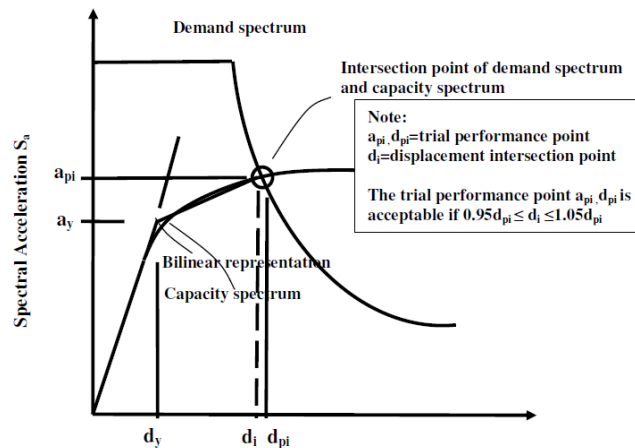


Figure 3.14: Estimation of target displacement using CSM method

3.5.9 Performance Point of MDOF System

When the performance point has been calculated, it is converted to the target displacement of the MDOF system using:

$$u_i = PF_1 \phi_{ij} S_d \quad (3.10)$$

Where PF_1 is the participation factor and S_d is the spectral displacement of the equivalent SDOF system. The strength of structural elements and story drifts can now be checked for the target displacement. If the capacity curve can extend through the envelope of the demand curve, the structure survives the earthquake. The intersection of the capacity and demand curve represents the force and displacement of the structure for that earthquake.

3.6 Strengthening the Building Using Shear Wall with Crushed Waste Tires

As mentioned in the previous problem statement, there is a need to rehabilitate a building with the least destructive intervention possible and also for the process to be economical and accessible for the existing building, using a shear wall system to strengthen the inadequate RC building is a good solution for strengthening, as well as stiffening the building for resisting lateral loads. To achieve the strengthening objectives that are ranging from drift control to collapse prevention, the shear wall used to retrofit the existing building has special characteristics in terms of its mix proportions. Moreover, 4 different mix proportions have been used, as shown in Tables 3.3 and their mechanical properties are shown in Tables 3.4 while one mix was used as normal concrete has characteristic strength equals to 30 MPa.

Table 3.3: Mix identifications and proportions of materials (kg/m³).

Mix ID	Cement	Course aggregate	Fine aggregate	Weight of Rubber Powder (kg/m ³)	Tire chips	Fine crumb rubber	Weight of Rubber chipped (kg/m ³)	Silica Fume (kg)	Steel Fiber (kg)
5TC5FCR (Gesoğlu et al., 2014)	450	1434.6	0	0	29.9	14.1	-	-	-
10% Powder rubber (Sofı, A. 2017)	342	927	858	38	-	-	-	-	-
10% aggregate rubber (Sofı, A. 2017)	380	839	858	-	-	-	93	-	-
High performance shear wall with 25RBC (Habib, A. 2019)	1000	504	336	-	-	-	117	300	78

Table 3.4: Mechanical properties of concrete replaced with waste rubber.

Mix ID	Compressive strength (MPa)	Splitting tensile strength (MPa)	Flexural tensile strength (MPa)	Elasticity moduli (GPa)
5TC5FCR (Gesoğlu et al., 2014)	13.20	0.81	-	8.2
10% Powder rubber (Sofı, A. 2017)	20	1.7	3.9	19
10% aggregate rubber (Sofı, A. 2017)	25	1.5	3.4	20
High performance shear wall with 25RBC (Habib, A. 2019)	55.07	4.88	4.39	36.6

During the shear wall installation period, a problem arose: initially, the ideal solution was to directly attach the shear wall to the existing skeleton of the structure because the existing building has cantilevers extruding 1.5 m in the edges. This type of

cantilever slab has a negative effect on the lateral displacement of the building during earthquake shaking. It was decided that this negative effect can be reduced if the shear walls are constructed inside the skeleton by removing the brick walls, as shown in Figure 3.15. After that, the shear wall had been modeled by a Mid-Pier Frame and plastic hinges defined for nonlinear analysis according to FEMA 356 on SAP2000 together with concrete frames and performance analysis done using the ATC-40 method in order to evaluate the results (Genets et al., 2015). The thickness of the shear walls can be considered as 0.25 m, but for 25% rubberized high performance concrete (25RBC), the width was 10 cm. The rebar distribution of the shear walls are given in Figure 3.16.



Figure 3.15: Infill shear wall (Akin, et al., 2016).

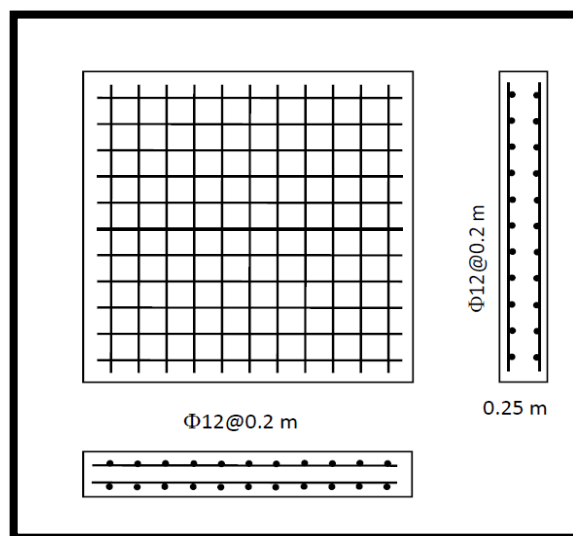


Figure 3.16: Reinforcement distribution in the shear wall.

Chapter 4

RESULTS AND DISCUSSION

4.1 Introduction

In the previous chapter, the creation of the 3D model of the building and the determination of the material properties were outlined. This chapter presents the seismic assessment and strengthening results of the existing building. The analysis was performed on the calibrated model by considering the dynamic parameters obtained from a forced vibration test and the contribution of the infill walls. The analysis is done using the capacity spectrum curves of the structure and demand curves of the earthquake. The performance points, obtained from the capacity spectrum method (CSM) of the structure, are used to estimate the hinges' state, which is subsequently used as a basis for strengthening the building. Four internal shear walls are used to retrofit the building in three different locations. The nominated shear wall is selected based on the stiffness that it provides to the building and the minimum amount of materials used to design it. After strengthening, the shear wall performance is simulated using CSM. All modeling and analyses were performed using SAP2000.

4.2 Details of the Modelling

The building was modeled using SAP2000 and the basic 3D model of the building was created from its original architectural plans. Moreover, the infill walls are considered as mass and the stiffness element as the compression strut in the model.

By considering the infill wall as mass in the modeling the total weight of the structure is 1293.14 Ton. Moreover, the changing in weight by removing some infill walls and constructing shear walls instead of infill walls the weight of the structure increased. For configurations shear wall-I, shear wall-II and shear wall-III the weight of the structure using normal concrete is 1359.62 Ton, 1374.14 Ton and 1378.36 Ton, respectively. Moreover, the changing in weight is increased around 7% and the dominant period of the structure 3% that change does not affect the performance of the structure considerably.

Table 4.1: Details of the model.

Model Properties	
Weight of structure	1293.14 Ton
Slab type	Solid
Thickness of slab	150 mm
Modulus of Elasticity	30000 MPa
Existing concrete compressive strength	25 MPa
Existing steel reinforcement tensile strength	220 MPa

According to original structure plans (see Figure A18 in the appendix) of the building the footings are single footing for each column. During the modeling of the structure, it is assumed that a strong enough footings are constructed and connected

to the single footings of the side columns of each shear wall. This assumption is one of the limitation of the study.

4.3 Model Calibration

The natural vibration frequency of the structure was determined based on the forced vibration test and presented in Table 3.1. The method that has been used to determine the modulus of elasticity is based on determination of vibration parameters of a building by using vibration generator. Applying modal analysis to a building in SAP2000 provides a theoretical prediction of the dynamic vibration behavior parameters, which can be compared to its real dynamic vibration parameters by changing the Modulus of Elasticity of the concrete in the model until the theoretical vibration period becomes equal or close to the real one obtained from the forced vibration test. Table 4.2 outlines the changes to the period and frequency of the model by changing the modulus of elasticity.

The building was modeled using SAP2000. The results of the vibration frequency test in SAP2000 report that the period of mode I is 0.46 and 0.45 for mode II without brick walls, which is reflected in the analytical period. Moreover, partition walls modelled as compression strut to reflect the realistic performance of the real building.

The infill walls are considered a compression strut in the model. By applying the aforementioned method, the modulus of elasticity of the building is obtained as 30000MPa. The periods obtained were 0.35 and 0.32, which are close to the period obtained from the forced vibration test.

Table 4.2: Period and frequency of the model

Modulus of elasticity (Mpa)	Mode	Without compression strut		With compression strut	
		Period (sec)	Frequency (Cyc/sec)	Period (sec)	Frequency (Cyc/sec)
20,000	1	0.59	1.44	0.46	1.71
	2	0.58	1.48	0.43	1.81
22,000	1	0.57	1.51	0.43	1.80
	2	0.56	1.55	0.4	1.90
24,000	1	0.55	1.58	0.41	1.88
	2	0.53	1.62	0.38	1.99
26,000	1	0.52	1.65	0.39	1.95
	2	0.51	1.68	0.36	2.07
28,000	1	0.51	1.71	0.37	2.03
	2	0.49	1.75	0.34	2.15
30,000	1	0.48	1.77	0.35	2.10
	2	0.47	1.81	0.32	2.22
32,000	1	0.46	1.83	0.34	2.17
	2	0.45	1.87	0.31	2.29
34,000	1	0.44	1.88	0.32	2.24
	2	0.43	1.93	0.3	2.37
36,000	1	0.43	1.94	0.31	2.30
	2	0.42	1.98	0.29	2.43
38,000	1	0.42	1.99	0.3	2.36
	2	0.4	2.04	0.27	2.50

4.4 Performance of the Building Before Strengthening

The performance of the building is evaluated for both directions (X and Y) without any strengthening using ATC-40 CSM. This method produces the target displacement and shear force curve, which is dependent on the level of expected seismic activity in Antakya, the soil properties of the site, effective mass in the first mode, and the viscous damping capacity of the existing building. The target displacement and shear force curve is obtained by transferring the shear force to spectral acceleration and the displacement to the spectral displacement so the performance curve can be compared to the demand curve. The performance point was obtained according to the capacity spectrum ATC-40 in X-direction, where shear

force is equal to 2262.642 kN and displacement equals 0.074 m, and in Y-direction where shear force is equal to 2240.436 kN and displacement equals 0.134 m, as shown in Figure 4.1 and 4.2.

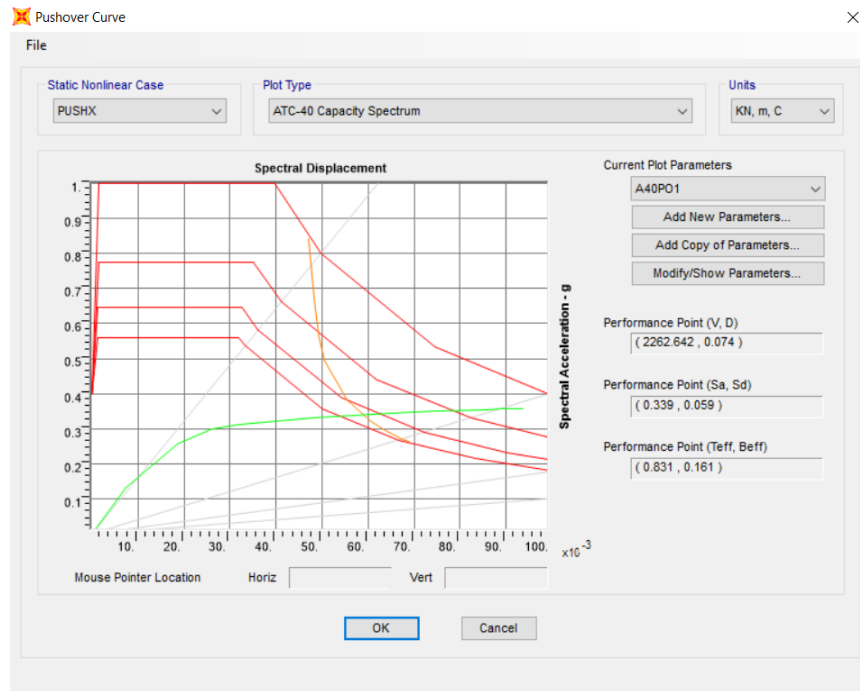


Figure 4.1: Demand and capacity spectrum in X-direction before strengthening.

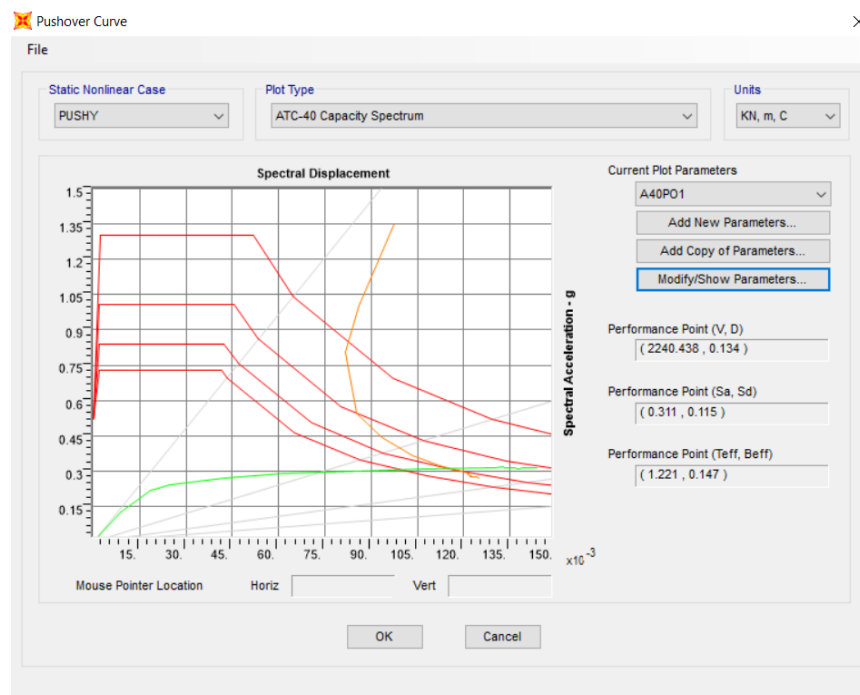


Figure 4.2: Demand and capacity spectrum in Y-direction before strengthening

After getting the performance point for each direction, a table is provided to evaluate the hinges' performance for each step. The performance point is compared with the base shear force from Table 4.3. In this case, the performance point is between step 5 and 6. As a conservative design, step 6 is chosen to be the critical point and was still in the immediate occupancy level. The same procedure has been done in the Y direction and step 19 is selected as the critical point, which was in collapse prevention level as shown in Table 4.4.

Table 4.3: Plastic hinges state in X-direction before strengthening.

TABLE: Pushover Capacity Curve												
LoadCase	Step	Displacement	BaseForce	AtoB	BtoIO	IOtoLS	LStoCP	CPtoC	CtoD	DtoE	BeyondE	Total
Text	Unitless	m	KN	Unitless	Unitless	Unitless	Unitless	Unitless	Unitless	Unitless	Unitless	Unitless
PUSHX	0	0.000044	0	750	0	0	0	0	0	0	0	750
PUSHX	1	0.010213	831.112	749	1	0	0	0	0	0	0	750
PUSHX	2	0.024377	1641.902	688	62	0	0	0	0	0	0	750
PUSHX	3	0.033322	1924.734	647	103	0	0	0	0	0	0	750
PUSHX	4	0.040241	2035.121	616	134	0	0	0	0	0	0	750
PUSHX	5	0.060406	2202.264	581	169	0	0	0	0	0	0	750
PUSHX	6	0.081431	2299.05	550	190	10	0	0	0	0	0	750
PUSHX	7	0.093447	2344.76	529	193	28	0	0	0	0	0	750
PUSHX	8	0.107107	2382.177	513	204	33	0	0	0	0	0	750
PUSHX	9	0.107136	2382.08	513	204	33	0	0	0	0	0	750
PUSHX	10	0.107524	2383.221	513	204	33	0	0	0	0	0	750
PUSHX	11	0.111363	2389.801	508	208	34	0	0	0	0	0	750
PUSHX	12	0.115919	2401.206	502	212	36	0	0	0	0	0	750
PUSHX	13	0.116082	2401.441	502	212	36	0	0	0	0	0	750
PUSHX	14	0.116834	2403.224	502	212	36	0	0	0	0	0	750
PUSHX	15	0.116916	2403.236	502	212	36	0	0	0	0	0	750
PUSHX	16	0.118347	2406.235	501	213	36	0	0	0	0	0	750

Table 4.4: Plastic hinges state in Y-direction before strengthening.

TABLE: Pushover Capacity Curve												
LoadCase	Step	Displacement	BaseForce	AtoB	BtoIO	IOtoLS	LStoCP	CPtoC	CtoD	DtoE	BeyondE	Total
Text	Unitless	m	KN	Unitless	Unitless	Unitless	Unitless	Unitless	Unitless	Unitless	Unitless	Unitless
PUSHY	0	0.000237	0	750	0	0	0	0	0	0	0	750
PUSHY	1	0.011876	816.587	748	2	0	0	0	0	0	0	750
PUSHY	2	0.023481	1440.129	693	57	0	0	0	0	0	0	750
PUSHY	3	0.030631	1633.513	651	99	0	0	0	0	0	0	750
PUSHY	4	0.05124	1888.749	609	141	0	0	0	0	0	0	750
PUSHY	5	0.072434	2034.795	575	152	23	0	0	0	0	0	750
PUSHY	6	0.099001	2147.309	557	140	53	0	0	0	0	0	750
PUSHY	7	0.124186	2217.395	536	135	79	0	0	0	0	0	750
PUSHY	8	0.146882	2268.34	517	129	104	0	0	0	0	0	750
PUSHY	9	0.150685	2273.79	515	129	105	0	0	1	0	0	750
PUSHY	10	0.15069	2271.747	511	133	105	0	0	1	0	0	750
PUSHY	11	0.154039	2285.085	509	130	110	0	0	1	0	0	750
PUSHY	12	0.154059	2248.856	509	130	110	0	0	0	1	0	750
PUSHY	13	0.154368	2251.535	509	128	112	0	0	0	1	0	750
PUSHY	14	0.1548	2254.012	509	128	112	0	0	0	1	0	750
PUSHY	15	0.157957	2263.431	508	126	113	0	0	2	1	0	750
PUSHY	16	0.157977	2251.695	508	126	113	0	0	2	1	0	750
PUSHY	17	0.158349	2255.692	508	126	113	0	0	2	1	0	750
PUSHY	18	0.158369	2228.522	508	126	113	0	0	0	3	0	750
PUSHY	19	0.159423	2241.259	504	126	113	0	0	0	7	0	750
PUSHY	20	0.16084	2251.788	504	126	113	0	0	0	7	0	750
PUSHY	21	0.163998	2262.18	503	125	115	0	0	0	7	0	750
PUSHY	22	0.166047	2266.005	501	124	117	0	0	0	8	0	750
PUSHY	23	0.166047	2266.005	501	124	117	0	0	0	8	0	750

Figures 4.3 and 4.4 show the hinge levels details at the last step of the pushover analysis in both directions.

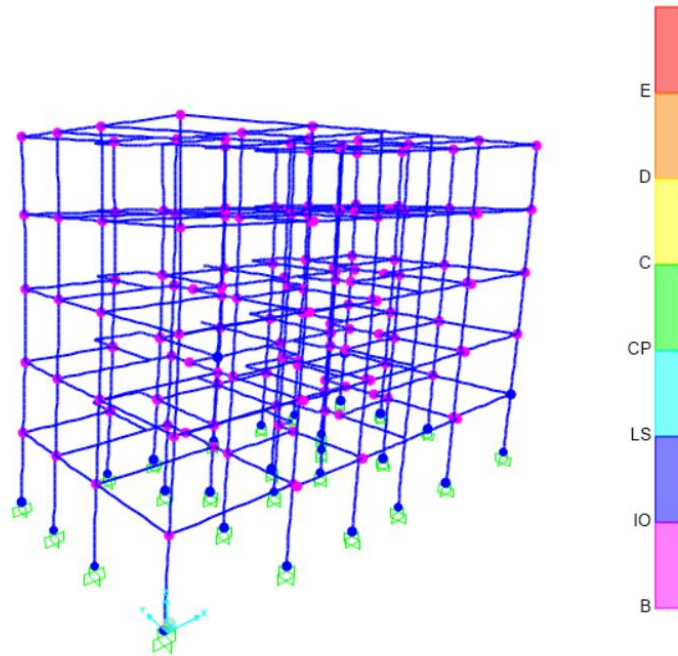


Figure 4.3: Hinges state in step 16 in X-direction.

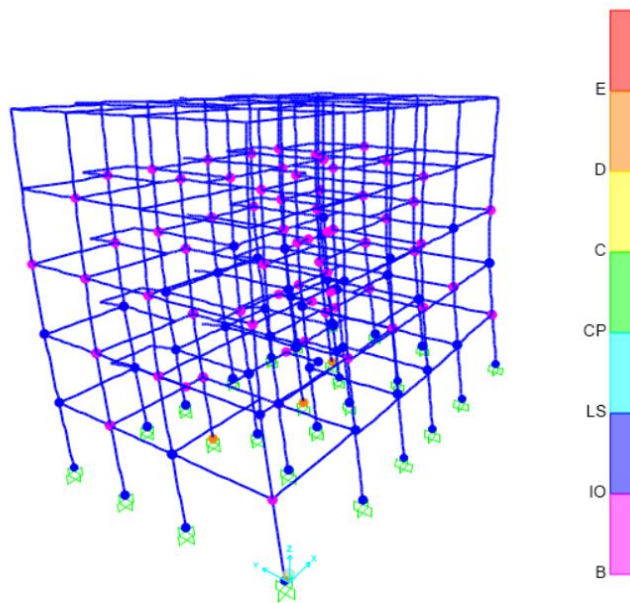


Figure 4.4: Hinges states in step 23 Y-direction.

After performing the pushover analysis and the Roof Displacement-Base Shear curve (Capacity Curve) is obtained, the ATC-40 for the selected performance level has to be determined. The strategy depicted in the TEC 2007 was mentioned in Chapter 3. As indicated by the TEC 2007 earthquake code specifications for the results of earthquake calculations applied on any floors, a maximum 10 % of the beams can exceed the Significant Damage Zone, while all other load-bearing components must remain in the Minimum Damage Zone. Such buildings are agreed to be in the Immediate Occupancy Level provided that the brittle damaged components, if any, are strengthened. For columns, the performance should satisfy the immediate occupancy according to TEC 2007 and the collapse should not be observed on columns bearing 30% of the shear force. Tables 4.5 - 4.8 summarize the results for the aforementioned nonlinear analysis procedure. As can be observed, the existing system of the building under consideration cannot satisfy the performance levels because 7 columns are in the collapse stage (Table 4.8).

Table 4.5: Immediate occupancy performance level in X-direction for beams in the existing structure.

Story	Total number of beams	Beam not satisfying performance Level		
		Number	ratio	check
Second	34	0	0.00	<10%
First	34	0	0.00	<10%
Ground	34	0	0.00	<10%

Table 4.6: Immediate occupancy performance level in X-direction for columns in the existing structure.

Story	Total number of columns	Column not satisfying performance Level		
		LS	CP	>C
Second	26	0	0	0
First	26	0	0	0
Ground	26	0	0	0

Table 4.7: Immediate occupancy performance level in Y-direction for beams in the existing structure.

Story	Total number of beams	Beam not satisfying performance Level		
		Number	ratio	check
Second	34	0	0.00	<10%
First	34	0	0.00	<10%
Ground	34	0	0.00	<10%

Table 4.8: Immediate occupancy performance level in Y-direction for columns in the existing structure.

Story	Total number of columns	Columns not satisfying performance Level		
		LS	CP	>C
Second	26	0	0	0
First	26	0	0	0
Ground	26	0	0	7

4.5 Performance of the Building After Strengthening

4.5.1 Strengthening by Shear Wall

One general solution to the low performance of an existing building involves removing some brick walls and constructing a shear walls in the weak direction. Shear walls were the most acceptable technique used to strengthen the flexural and shear strength of the existing building. The building's ductility and stiffness increase, while the cost of strengthening decreases. Three different shear wall configurations are used to determine the optimal shear wall in terms of ductility and cost. The shear walls have modelled as mid-pier frame with plastic hinges in the core of frame of building. The observed weak direction (Y-direction) of the existing RC building has been retrofitted using five mix proportions of concrete for shear walls constructed with crushed tire rubber.

First configuration: The location of shear wall-I is shown in Figure 4.5. Moreover, the shear wall is constructed in the core of the frame of the building. The shear walls are selected according to several pushover runs to obtain a safe and also minimal section in order to decrease the cost.

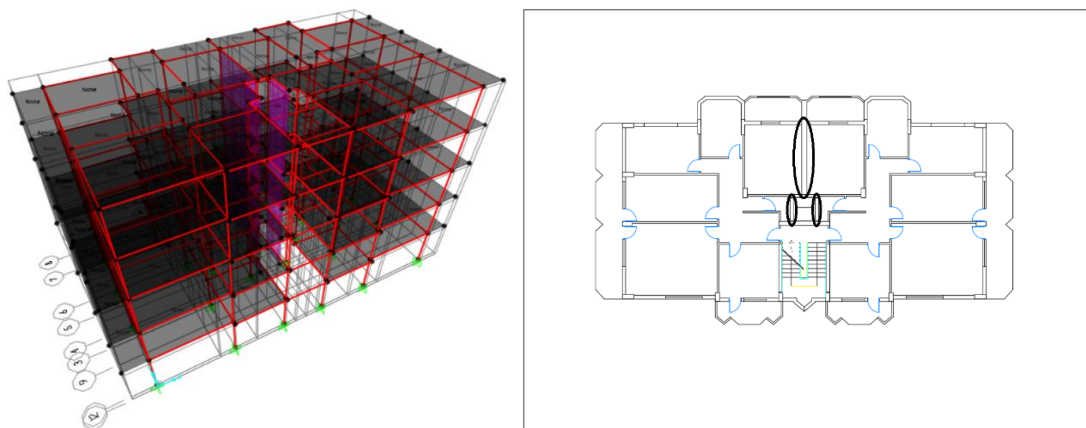


Figure 4.5: First shear wall configuration used for strengthening (shear wall-I).

Second configuration: Shear wall-II is located as shown in Figure 4.6. The shear wall was modeled using a mid-pier frame with plastic hinges in the core of the frame of the building.

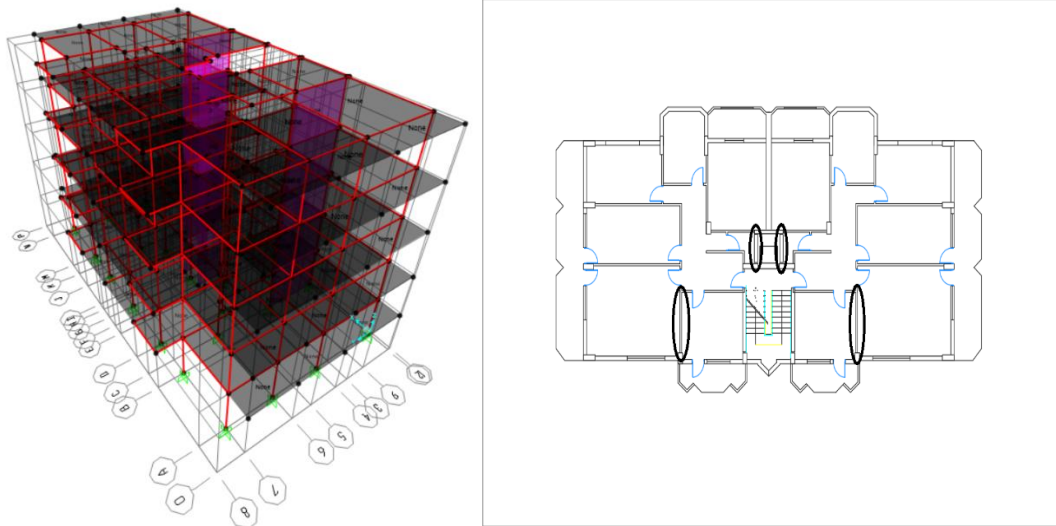


Figure 4.6: Second shear wall configuration used for strengthening (shear wall-II).

Third configuration: Shear wall-III is located as shown in Figure 4.7.

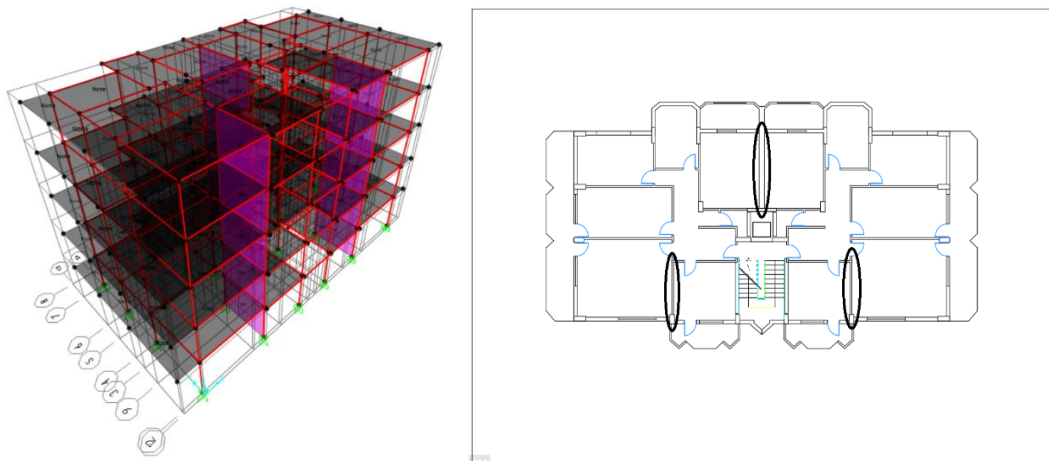


Figure 4.7: Third shear wall configurations used for strengthening (shear wall-III).

4.5.2 Performance in X-Direction after Strengthening

After strengthening in X-direction, the load in the capacity spectrum curve increased from 2202.64 kN to 2363.18 kN and the displacement decreased from 0.074 m to 0.051 m using a normal shear wall, as shown in Table 4.9. Shear wall-III has the capability to take a higher shear force and displacement than Shear wall-I and Shear wall-II, as is also shown in Table 4.9. There is a slight increase in the performance of the building in X-direction because the shear wall was installed in Y-direction.

Table 4.9: Performance points for frames with and without shear walls (X-Direction).

	Configuration	Shear Force (kN)	Displacement (m)
Without shear wall		2202.64	0.074
Normal shear wall	Shear wall-I	2314.35	0.059
	Shear wall-II	2347.28	0.056
	Shear wall-III	2363.18	0.051
Shear wall with 5TC5FCR (Gesoglu et al., 2014)	Shear wall-I	2241.54	0.071
	Shear wall-II	2258.48	0.069
	Shear wall-III	2266.46	0.064
Shear wall with 10% Powder rubber(Sofi, A. 2017)	Shear wall-I	2283.69	0.062
	Shear wall-II	2297.24	0.061
	Shear wall-III	2304.87	0.059
Shear wall with 10% aggregate rubber(Sofi, A. 2017)	Shear wall-I	2294.27	0.060
	Shear wall-II	2306.87	0.058
	Shear wall-III	2312.42	0.054
High performance shear wall with 25RBC (Habib, A. 2019)	Shear wall-I	2641.82	0.042
	Shear wall-II	2673.71	0.038
	Shear wall-III	2697.28	0.033

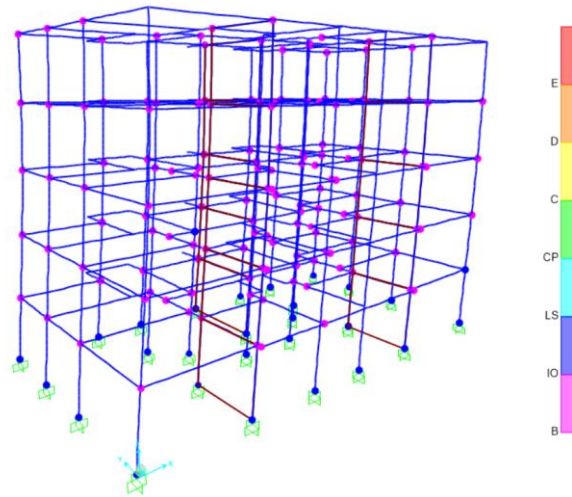


Figure 4.8: Hinges' state in step 14 in X direction (Normal shear wall – Shear wall-III)

Figure 4.8 shows the hinges' state for each member of the model. As seen from the figure, some hinges are in the yield level while others are in immediate occupancy.

Table 4.10 illustrates the hinges' state in the model before and after strengthening.

Table 4. 10: Hinges state before and after strengthening in X-direction

	Configuration	IO	LC	CP
Without shear wall		190	0	0
Normal shear wall	Shear wall-I	147	0	0
	Shear wall-II	156	0	0
	Shear wall-III	163	0	0
Shear wall with 5TC5FCR (Gesoglu et al., 2014)	Shear wall-I	118	0	0
	Shear wall-II	124	0	0
	Shear wall-III	129	0	0
Shear wall with 10% Powder rubber(Sofi, A. 2017)	Shear wall-I	137	0	0
	Shear wall-II	148	0	0
	Shear wall-III	151	0	0
Shear wall with 10% aggregate rubber(Sofi, A. 2017)	Shear wall-I	149	0	0
	Shear wall-II	151	0	0
	Shear wall-III	159	0	0
High performance shear wall with 25RBC (Habib, A. 2019)	Shear wall-I	157	0	0
	Shear wall-II	169	0	0
	Shear wall-III	175	0	0

4.5.3 Performance in Y-Direction after Strengthening

After strengthening in Y-direction, the load in the capacity spectrum curve increased from 2240.436 kN to 2873.19 kN and the displacement decreased from 0.134 to 0.082 using a normal shear wall. In this direction, as was expected, the capacity spectrum curve experienced a significant increase in performance points. The performance points are shown in Table 4.11 before and after strengthening. The hinges' state for each member of the frame is given in Figure 4.9 using a normal shear wall-III.

Table 4.11: Performance points for both frames with and without the shear wall (Y-Direction)

	Configuration	Shear Force (kN)	Displacement (m)
Without shear wall		2240.43	0.134
Normal shear wall	Shear wall-I	2789.47	0.09
	Shear wall-II	2843.72	0.086
	Shear wall-III	2873.19	0.082
Shear wall with 5TC5FCR (Gesoglu et al., 2014)	Shear wall-I	2472.65	0.113
	Shear wall-II	2523.41	0.109
	Shear wall-III	2595.77	0.102
Shear wall with 10% Powder rubber(Sofi, A. 2017)	Shear wall-I	2657.24	0.109
	Shear wall-II	2679.73	0.098
	Shear wall-III	2698.74	0.094
Shear wall with 10% aggregate rubber(Sofi, A. 2017)	Shear wall-I	2683.27	0.099
	Shear wall-II	2697.18	0.097
	Shear wall-III	2734.84	0.091
High performance shear wall with 25RBC (Habib, A. 2019)	Shear wall-I	3047.84	0.077
	Shear wall-II	3101.05	0.073
	Shear wall-III	3143.72	0.068

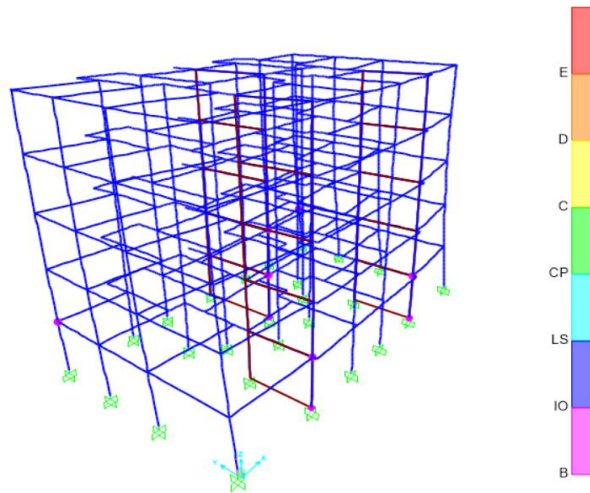


Figure 4.9: Hinges' state in step 12 in Y-direction (Normal shear wall – Shear wall-III)

In both directions X and Y, the hinges' state is within the immediate occupancy range, as shown in Tables 4.9 and 4.11. As a result shear wall-III is the most efficient than the shear wall configurations I and II as shown in Table 4.10.

Table 4.12: Hinges states in Y-direction

	Configuration	IO	LC	CP
Without shear wall		113	21	7
Normal shear wall	Shear wall-I	156	11	0
	Shear wall-II	153	9	0
	Shear wall-III	143	6	0
Shear wall with 5TC5FCR (Gesoglu et al., 2014)	Shear wall-I	140	18	0
	Shear wall-II	138	16	0
	Shear wall-III	130	12	0
Shear wall with 10% Powder rubber(Sofi, A. 2017)	Shear wall-I	139	13	0
	Shear wall-II	134	10	0
	Shear wall-III	128	9	0
Shear wall with 10% aggregate rubber(Sofi, A. 2017)	Shear wall-I	140	10	0
	Shear wall-II	136	9	0
	Shear wall-III	132	8	0
High performance shear wall with 25RBC (Habib, A. 2019)	Shear wall-I	121	9	0
	Shear wall-II	119	7	0
	Shear wall-III	117	6	0

In both directions X and Y, the hinges' state is within the immediate occupancy range, as shown in Tables 4.10 and 4.12. As a result, the location of shear wall-III is more efficient than shear wall configurations I and II as shown in Table 4.9 and Table 4.11. Moreover, the result of strengthening the residential building was immediate occupancy, which is a very high degree of strengthening for a residential building. However, the reason behind this is that the building is already existing and a shear wall must be built between two columns but it is not possible to build it in the case of a short distance between two columns because this leads to a short beam, which is not designed as such.

4.6 Comparative Demand and Capacity Spectrum for X and Y-Direction Before and After Strengthening

The performance points were obtained using the capacity curves and the procedure defined in the TEC 2007. Before the strengthening, the performance points were found at a shear force of 2202.64 kN and at a displacement equal to 0.074 m in X-direction and at a shear force of 2240.436 kN and a displacement equal to 0.134 m in the Y-direction (Table 4.10).

As a result of the analysis, the location of shear wall-III is suggested to be more efficient than the locations of shear wall-I and shear wall-II. Moreover, the performance point was obtained using different mix proportions at a shear force of 2873.19 kN and a displacement equal to 0.082 for the normal shear wall. However, when 10% of the cement is replaced with rubber powder, the shear force equals 2698.74 and the displacement equals 0.094. Moreover, the location of Shear wall-III showed the highest performance, although, the performance points showed a significant improvement in both X-and Y-directions.

4.7 Comparison of the Cost Estimations Between Different Types of Concrete Mixtures Including Waste Tire Rubber

The recycling of waste tires is of paramount importance for environmental protection and for economic reasons. Tables 4.13, 4.14 and 4.15 are shown the cost price result of cost estimations, the location of shear wall-I has the least use of concrete; since only 27.25 m³ of concrete was used to build the shear wall, the costs of construction will be the lowest. When comparing the five mixtures, it can be found that the production cost of replacing 10% of the coarse aggregate with waste rubber is 9020 TL which is the lowest cost. Moreover, the Shear wall with 10% Powder rubber is the highest cost comparing with the same shear wall configuration and its cost 11172 TL. The highest volume of concrete are used in third shear wall configurations with 35.5 m³.

Table 4.13: Cost price of the second shear wall configurations.

Shear wall-I	Concrete (m ³)	Unite price (TL)	Total cost (TL)
Normal shear wall	27.25	360	9810
Shear wall with 5TC5FCR	27.25	348	9483
Shear wall with 10% Powder rubber	27.25	410	11172
Shear wall with 10% aggregate rubber	27.25	331	9020
Shear wall with high performance concrete 25RBC	16.43	625	10268

Table 4.14: Cost price of the second shear wall configurations

Shear wall-II	Concrete (m ³)	Unite price (TL)	Total cost (TL)
Normal shear wall	33.75	360	12150
Shear wall with 5TC5FCR	33.75	348	11745
Shear wall with 10% Powder rubber	33.75	410	13837
Shear wall with 10% aggregate rubber	33.75	331	11171
Shear wall with high performance concrete 25RBC	20.25	625	12656

Table 4.15 Cost price of the third shear wall configurations

Shear wall-III	Concrete (m ³)	Unite price (TL)	Total cost (TL)
Normal shear wall	35.5	360	12780
Shear wall with 5TC5FCR	35.5	348	12354
Shear wall with 10% Powder rubber	35.5	410	14555
Shear wall with 10% aggregate rubber	35.5	331	11750
Shear wall with high performance concrete 25RBC	21.37	625	13356

Chapter 5

CONCLUSION AND RECOMMENDATIONS

5.1 Summary

The aim of this study is to provide a procedure for building performance evaluation and strengthening that is fast, cheap, reliable and environmental friendly. The main parameters that have been considered in this study are: strengthening with minimum interference for building residents, minimum required damage to the building, and minimum strengthening cost. The procedure has been tested on a residential apartment built in 1988. The building is a five-story RC apartment, located in Antakya, Turkey. The study has been conducted by utilizing distinctive codes and a diverse investigative methodology in its examination.

The material properties of the building were obtained by coupling real vibration record results with the building model in SAP2000. The material properties and other parameters were used to evaluate the building's performance. The method which has been used for building performance evaluation is a pushover analysis (nonlinear elastic analysis). The performance point is calculated before and after strengthening using CSM and is used to assess the structural system. Based on the building's performance, some of the hinges were found to have reached the collapse level. As a result, the building structure was strengthened using three shear wall configurations.

5.2 Conclusion

This study was conducted to provide a fast, cheap, and reliable procedure for evaluating and strengthening an existing building. The main conclusions are:

- The modulus of elasticity was obtained as 30000 MPa using model calibrations with real vibration data. The main advantages of this method are:
 - It is a non-destructive method that requires no damage to the building with minimum interference for building residents.
 - The modulus of elasticity represents the overall value of the building compared to other methods that use local material properties.
 - It accounts for all of the building's structural defects, such as construction errors.
- The structure's evolution before strengthening showed that the building is near collapse based on the Turkish Earthquake Code (TEC2007). The results showed that the performance level in X-Direction is in an immediate occupancy level, while 7 hinges in Y-Direction are at collapse level. For this reason, strengthening was suggested.
- Three infill shear walls constructed with concrete has mixture of crushed waste rubber as a replacing material for four different mixtures obtained from three different studies (Gesoglu et al., 2014; Safi, A. 2017; Habib, A., 2019) based on mechanical properties of concrete. The main advantage of using an infill shear walls are that they requires minimum interference with the building's residents and minimum building damage.
- The same evaluation method was applied after strengthening. The results showed that all-plastic hinges' performance levels in Y-direction increased to

the immediate occupancy level as required by the Turkish Earthquake Code (TEC 2007).

- The study showed that the infill shear wall does not need to be for the X direction of the skeleton because the building is stiff enough and there is no collapse in this direction.
- Using only shear walls constructed with concrete has mixture of fine or coarse aggregate could provide enough strength and ductility with a reasonable cost.

5.3 Recommendations for Further Studies

It is expected that this study will be useful for the other private structures in Antakya city or other cities with a similar building stock in Turkey. If the work will be done to retrofit the existing buildings, the proposed technique would require the short-term evacuation of the residents from the apartments. Because of this advantage, other buildings can and should be investigated using the same methodology to determine their existing performance level. If they do not satisfy the required performance level according to the TEC 2007 or Turkey Building Earthquake Code (TBEC) 2018, the buildings should be strengthened using this proposed simple and time-saving and economical method.

REFERENCES

- Abdi, H., Hejazi, F., Jaafar, M. S., & Karim, I. A. (2016). Evaluation of response modification factor for steel structures with soft story retrofitted by viscous damper device. *Advances in Structural Engineering*, 19(8), 1275-1288.
- Akın, E., Korkmaz, S. Z., Korkmaz, H. H., & Diri, E. (2016). Rehabilitation of infilled reinforced concrete frames with thin steel plate shear walls. *Journal of Performance of Constructed Facilities*, 30(4), 04015098.
- Alhashimi, A. (2018). Seismic Assessment and Strengthening of Existing RC Building by Using Steel Braced Frames. *A Master Thesis in Civil Engineering*, Eastern Mediterranean University, Famagusta, Cyprus.
- Alam, I., Mahmoud, U. A., & Khattak, N. (2015). Use of Rubber as Aggregate in Using Concrete: A Review. *International Journal of Advanced Structures and Geotechnical Engineering*, 4(02).
- Army, U. S. (1986). Seismic design guidelines for essential buildings. *Departments of the Army* (TM-809-10-1), the Navy (NAVFAC P355. 1), and the Air Force AFM 88, 3.
- Ashraf Habibullah, S. E., & Stephen Pyle, S. E. (1998). Practical three dimensional the nonlinear static pushover analysis. *Structure magazine*, winter.d

- ATC-40 (1996). Seismic Analysis Retrofit of Concrete Buildings. Vol. I, Applied Technology Council, Redwood City, CA, USA.
- Badoux, M., & Jirsa, J. O. (1990). Steel bracing of RC frames for seismic strengthening. *Journal of Structural Engineering*, 116(1), 55-74.
- Baran, M. (2005). Precast concrete panel reinforced infill walls for seismic Technology strengthening of reinforced concrete framed structures. *A Doctor of Philosophy Thesis in Civil Engineering, Middle East Technical University, Ankara.*
- Batayneh, M. K., Marie, I., & Asi, I. (2008). Promoting the use of crumb rubber concrete in developing countries. *Waste management*, 28(11), 2171-2176.
- Belal, M.F., Mohamed H.M., and Morad S.A. 2014. "Behavior of reinforced concrete columns strengthened by steel jacket". *HBRC Journal*. 11 (2): 201-212
- Bush, T. D., Jones, E. A., & Jirsa, J. O. (1991). Behavior of RC frame strengthened using structural steel bracing. *Journal of Structural Engineering*, 117(4), 1115-1126.
- Chalioris, C. E., & Pourzitidis, C. N. (2012). Rehabilitation of shear-damaged reinforced concrete beams using self-compacting concrete jacketing. *ISRN Civil Engineering*, 2012.

- Choi, E., Chung, Y. S., Park, J., & Cho, B. S. (2010). Behavior of Reinforced Concrete Columns Confined by New Steel-Jacketing Method. *ACI Structural Journal*, 107(6).
- Council, Building Safety, (2000). Pre-standard and Commentary for the Seismic Rehabilitation of Building, Report FEMA-356, Washington, DC.
- Deierlein, G. G., Hsieh, S. H., & Shen, Y. J. (1990, March). Computer-Aided Design of Steel Structures with Flexible Connections. In *Proceedings of the 1990 National Steel Construction Conference, March 14-17, 1990, Kansas City, MO*.
- Eldin, N. N., & Senouci, A. B. (1993). Rubber-tire particles as concrete Steel Structures aggregate. *Journal of materials in civil engineering*, 5(4), 478-496.
- EM-DAT (Emergency Events Database) (2017).
- Elnashai, A. S. (2001). Advanced inelastic static (pushover) analysis for earthquake applications. *Structural engineering and mechanics*, 12(1), 51-70.
- Fattuhi, N.I., Clark, L.A., 1996. Cement-based materials containing shredded scrap truck tyre rubber. *Constr. Build. Mater.* 10 (4), 229e236.
- Genes, M, C Murat B, Sahin B (2011). *Full-Scale Dynamic Testing Of A RC Frame Building By Investigation The Effect Of Brick-Infilled Frames*. International Civil Engineering & Architecture Symposium for Academicians.

- Gesoğlu, M., Güneyisi, E., Khoshnaw, G., & İpek, S. (2014). Investigating properties of pervious concretes containing waste tire rubbers. *Construction and Building Materials*, 63, 206-213.
- Güneyisi, E., Gesoğlu, M., & Özturan, T. (2004). Properties of rubberized concretes containing silica fume. *Cement and concrete research*, 34(12), 2309-2317.
- Habib, A. (2019). Experimental and Analytical Study on the Structural Performance of RC Frame Strengthened with High Energy Dissipating Concrete Jacket. A *Master Thesis in Civil Engineering*, Eastern Mediterranean University, Famagusta, Cyprus.
- Han, Z., Chunsheng, L., Kombe, T., & Thong-On, N. (2008). Crumb rubber blends in noise absorption study. *Materials and Structures*, 41(2), 383-390.
- He, A., Cai J., Chen Q.J., Liu X., and Xu J. 2016. "Behaviour of steel-jacket retrofitted RC columns with preload effects". *Thin-Walled Structures*. 109: 25-39.
- Jeyasehar, C. A., Kumar, K. S., Muthumani, K., & Lakshmanan, N. (2009). Seismic performance evaluation methodologies for civil engineering structures. *Indian Journal of Engineering & Materials Sciences* 220-228.
- Kang, J., & Jiang, Y. (2008). Improvement of cracking-resistance and flexural behavior of cement-based materials by addition of rubber particles. *Journal of Wuhan University of Technology-Mater. Sci. Ed.*, 23(4), 579-583.

- Kaplan, H., Yilmaz, S., Cetinkaya, N., & Atimtay, E. (2011). Seismic strengthening of performance evaluation methodologies for civil engineering structures. Indian RC structures with exterior shear walls. *Sadhana*, 36(1), 1
- Karayannis, C. G., & Sirkelis, G. M. (2008). Strengthening and rehabilitation of RC beam–column joints using carbon-FRP jacketing and epoxy resin injection. *Earthquake Engineering & Structural Dynamics*, 37(5), 769-790.
- Kegyes-Brassai, O. K., & Ray, R. P. (2016). Earthquake Risk Assessment–Effect of a Seismic Event in a Moderate Seismic Area. *Acta Technica Jaurinensis*, 9(1), 1-15
- Khaloo, A. R., Dehestani, M., & Rahmatabadi, P. (2008). Mechanical properties of concrete containing a high volume of tire–rubber particles. *Waste management*, 28(12), 2472-2482.
- Khatib, Z. K., & Bayomy, F. M. (1999). Rubberized Portland cement concrete. *Journal of materials in civil engineering*, 11(3), 206-213.
- Krawinkler H. and Seneviratna G.D.P.K., 1998, *Pros and Cons of a Pushover of Analysis of Seismic Performance Evaluation*, Engineering Structures, Vol.20, 452-464
- Krawinkler, H., & Seneviratna, G. D. P. K. (1998). Pros and cons of a pushover analysis of seismic performance evaluation. *Engineering structures*, 20(4-6), 452-464.

- Lai, M.H., and Ho J.C.M. 2015. "Axial strengthening of thin-walled concrete-filled-steel tube columns by circular steel jackets". *Thin-Walled Structures*. 97: 11-21.
- Li, W., Wang, X., & Zhang, J. (2012). An Overview of the Study and Application of Rubberized Portland Cement Concrete. *Advanced Materials Research*.
- Liping, L., Kui, X., & Xuan, C. (2008). The research of applied pushover method in the earthquake resistance analysis of soil-structure interaction system. In *Proceedings of The Seminar on The 14th World Conference on Earthquake Engineering*.
- Mahaney, J. A., Paret, T. F., Kehoe, B. E., Freeman, S. A., & US Central United States Earthquake Consortium. (1993). the capacity spectrum method for evaluating structural response during the Loma Prieta earthquake. In *< 1993= Mil novecientos noventa y tres> National Earthquake Conference: Earthquake Hazard Reduction in the Central and Eastern United States: A Time for Examination and Action* (pp. 501-10). US Central United States Earthquake Consortium (CUSEC).
- Mainstone, R.J., on the stiffness and strength of infilled frames. *Proceedings of The Institute of Civil Engineers*, 4: 57–90, London, England, (1971).
- Marie, I., & Quiasrawi, H. (2012). Closed-loop recycling of recycled concrete Institute aggregates. *Journal of Cleaner Production*, 37, 243-248.

- Marlapalle, V. C., Salunke, P. J., & Gore, N. G. (2014). Analysis & design of RCC jacketing for buildings. *International Journal of Recent Technology and Engineering*, 3(3), 62-63.
- M-DAT (Emergency Events Database) (2017). www.emdat.be (last accessed on 24 Jan. 2017).
- Minafò, G. (2015). A practical approach for the strength evaluation of RC columns reinforced with RC jackets. *Engineering Structures*, 85, 162-169.
- Mosalam, K. M., & Naito, C. J. (2002). Seismic evaluation of gravity-load-designed column-grid system. *Journal of Structural Engineering*, 128(2), 160-168.
- Munshi, J. A., & Ghosh, S. K. (1998). Analyses of seismic performance of a code designed reinforced concrete building. *Engineering structures*, 20(7), 608-616.
- Mwafy, A. M., & Elnashai, A. S. (2002). Calibration of force reduction factors of RC buildings. *Journal of earthquake engineering*, 6(02), 239-273.
- Nagaprasad, P., Sahoo D.R., and Rai D.C. 2009. "Seismic strengthening of RC columns using external steel cage". *Earthquake Engineering & Structural Dynamics*. 38 (14): 1563-1586.
- Oikonomou, N., & Mavridou, S. (2009). The use of waste tyre rubber in civil engineering works. *In Sustainability of construction materials* (pp. 213-238). Woodhead Publishing.

- Onat, O., Yön, B., & Calayır, Y. (2018). Seismic assessment of existing RC buildings before and after shear-wall strengthening. *Gradevinar*, 70(08.), 703-712.
- Özşahin, E., & Değerliyurt, M. (2013). Modeling of Seismic Hazard Risk Analysis in Antakya (Hatay, South Turkey) by Using GIS. *International Journal of Innovative Environmental Studies Research*, 1(3), 31-54.
- Poursha, M., Khoshnoudian, F., & Moghadam, A. S. (2009). A consecutive modal pushover procedure for estimating the seismic demands of tall buildings. *Engineering Structures*, 31(2), 591-599.
- Prakash, A., & Thakkar, S. K. (2003). A comparative study of strengthening of RC building. In *Workshop on strengthening of structures, IIT Roorkee* (pp. 159-173).
- Sezen, H., and Miller E. 2011. "Experimental evaluation of axial behavior of strengthened circular reinforced-concrete columns". *ASCE Journal of Bridge Engineering*. 16 (2): 238-247.
- Shu, X., & Huang, B. (2014). Recycling of waste tire rubber in asphalt and portland cement concrete: An overview. *Construction and Building Materials*, 67, 217-224.
- Siddique, R., & Naik, T. R. (2004). Properties of concrete containing scrap-tire rubber—an overview. *Waste management*, 24(6), 563-569.

- Siddique, R., & Naik, T. R. (2004). Properties of concrete containing scrap-tire rubber—an overview. *Waste management*, 24(6), 563-569.
- Silva, V. and others (2014). Development of the OpenQuake engine, the Global Earthquake Model's open-source software for seismic risk assessment. *Natural Hazards*, 72(3), 1409-1427.
- Su, H., Yang, J., Ling, T., Ghataora, G. S., & Dirar, S. (2015). Properties of concrete prepared with waste tyre rubber particles of uniform and varying sizes. *Journal of Cleaner Production*, 91, 288-296. doi:10.1016/j.jclepro.2014.12.022.
- Tahsiri, H., Sedehi, O., Khaloo, A., & Raisi, E. M. (2015). Experimental study of RC jacketed and CFRP strengthened RC beams. *Construction and Building Materials*, 95, 476-485.
- TEC 2007, (2007). Turkish Earthquake Code: Regulation on Structures Constructed in Disasters Region. Ministry of Public Works and Settlements, Ankara, Turkey.
- Topçu, İlker. (1997). Assessment of the brittleness index of rubberized concretes. *Cement and Concrete Research*. 27. 177-183. 10.1016/S0008-8846(96)00199-8.
- Toutanji, H. A. (1996). The use of rubber tire particles in concrete to replace mineral aggregates. *Cement and Concrete Composites*, 18(2), 135-139.

- Vijayakumar, A., & Babu, D. V. (2012). Pushover analysis of existing reinforced concrete framed structures. *European Journal of Scientific Research*, 71(2), 195-202.
- Xiao, Y., and Wu H. 2003. "Retrofit of reinforced concrete columns using partially stiffened steel jackets". *Journal of Structural Engineering*. 129 (6).
- Yepes-Estrada, C. and V. Silva (2017). Probabilistic seismic risk assessment of the residential building stock in South America. *Proceedings of the 16th World Conference on Earthquake Engineering, 9-13 January 2017, Santiago*.
- Zborowski, A., Sotil Chávez, A., Kaloush, K., & Way, G. (2004). Material characteristics of asphalt rubber mixtures. *In Proceedings of the Asphalt Rubber 2003 Conference: Progress through flexibility*, Brasilia, Brasil. Distrito Federal. Departamento de Estradas de Rodagem (Brasília, Brasil).
- Zhang, F., Liu, Z., Qiu, K., Zhang, W., Wu, C., & Feng, S. (2015). Conductive rubber based flexible metamaterial. *Applied Physics Letters*, 106(6), 06190.
- Zine, A., Kadid, A., Lahbari, N., & Fourar, A. (2007). Pushover analysis of reinforced concrete structures designed according to the Algerian code. *Journal of Engineering and Applied Sciences*, 2(4), 733-738.

APPENDIX

Appendix: Data Collection of Studied Building

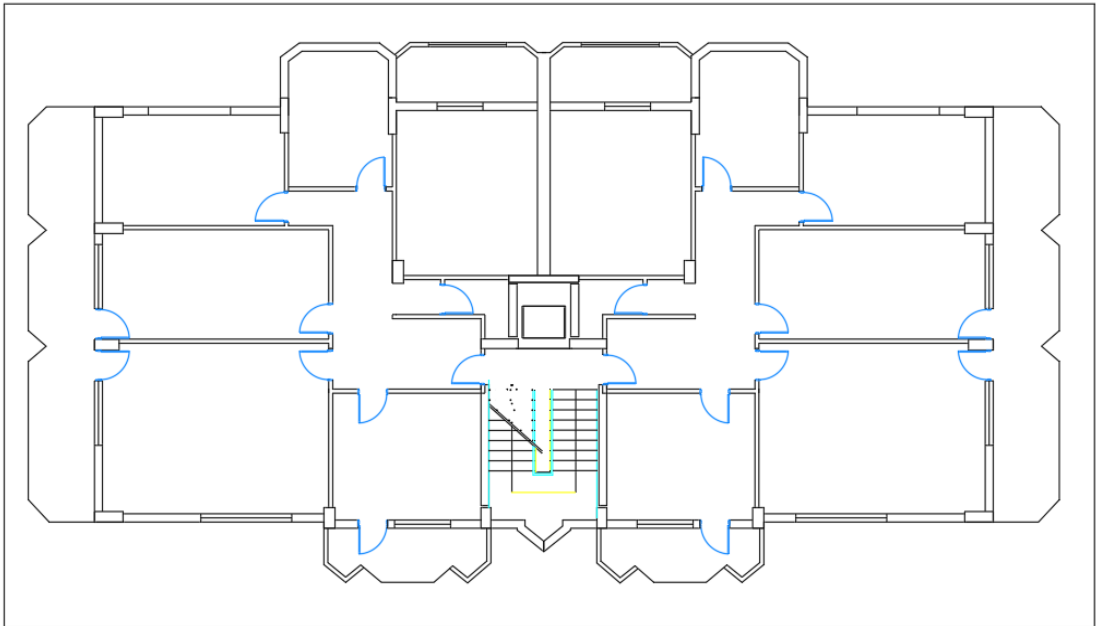


Figure A1: Plan of studied building

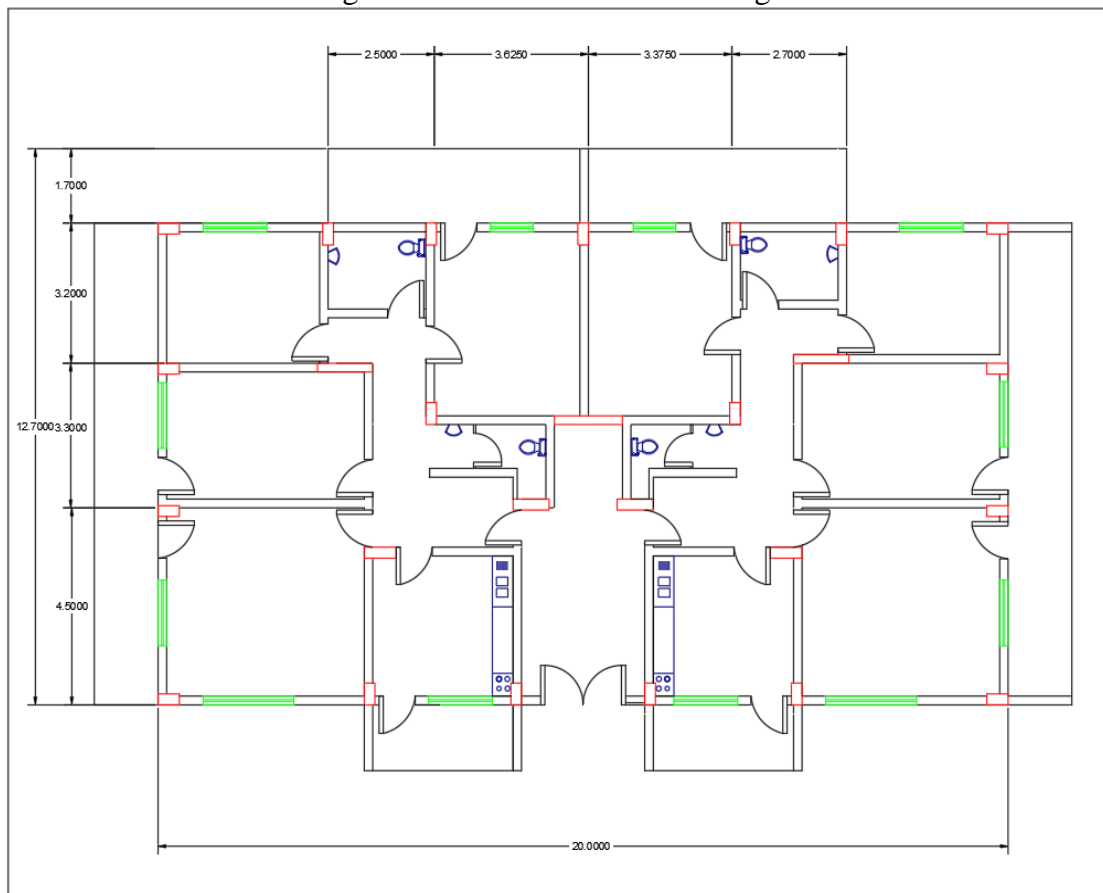


Figure A2: Grand floor of the studied building

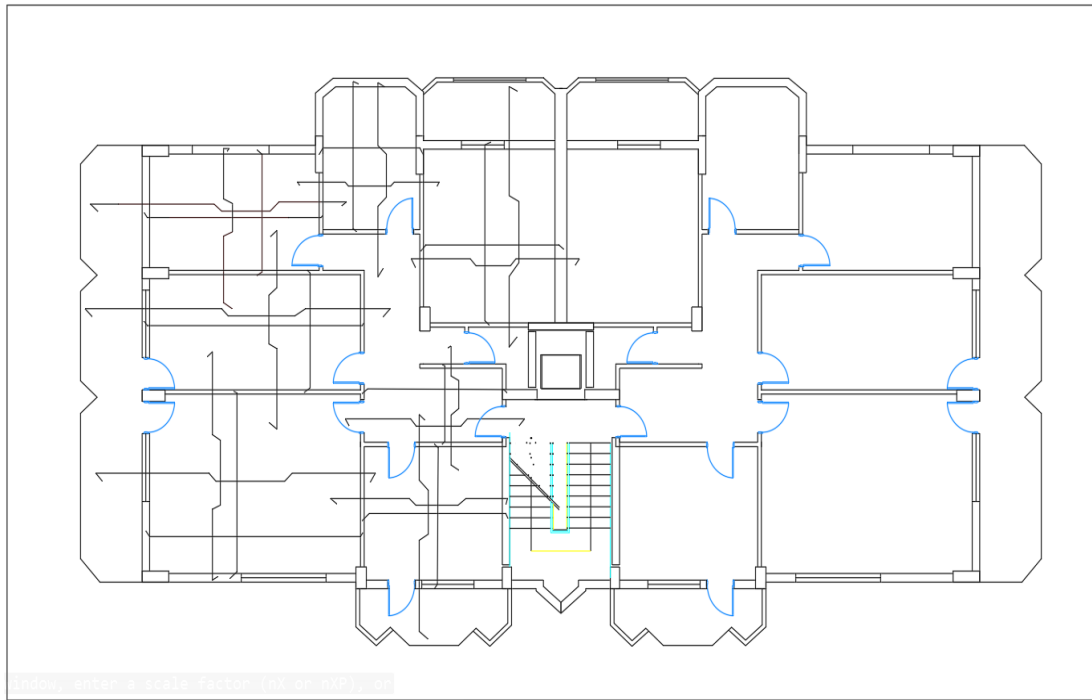


Figure A3: Reinforcement rebar of slab of the studied building

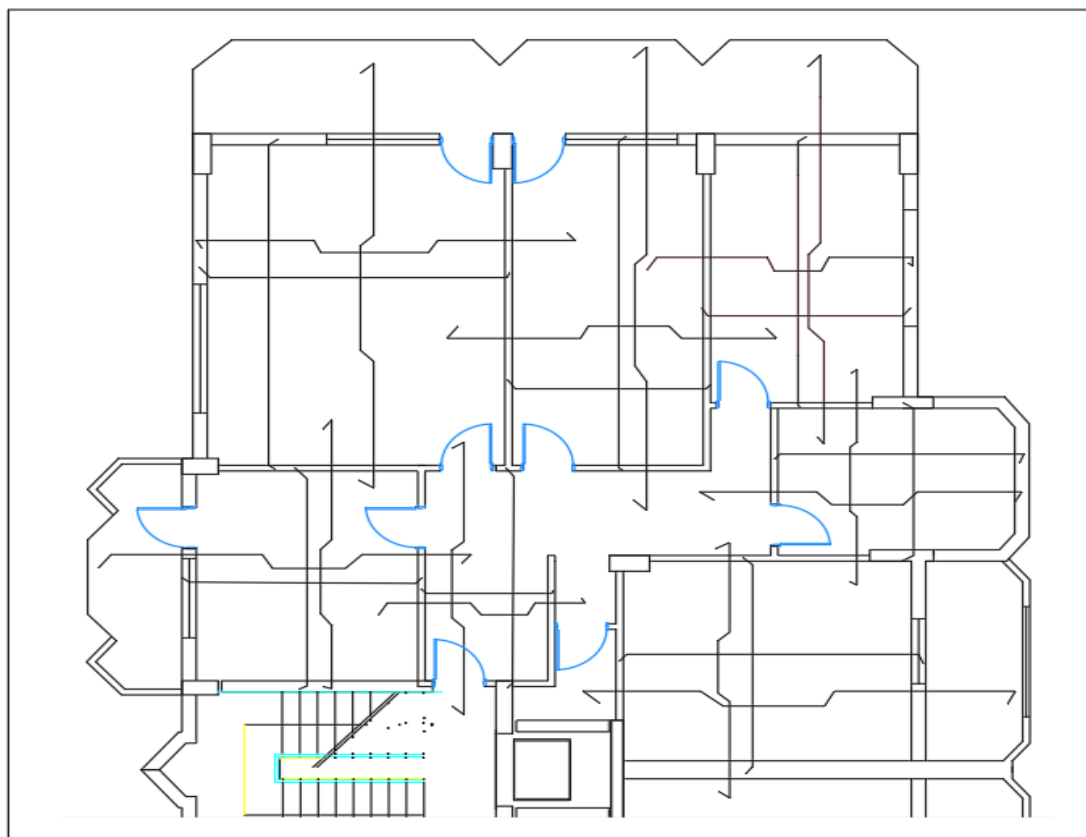


Figure A4: Reinforcement rebar of slabs of the studied building

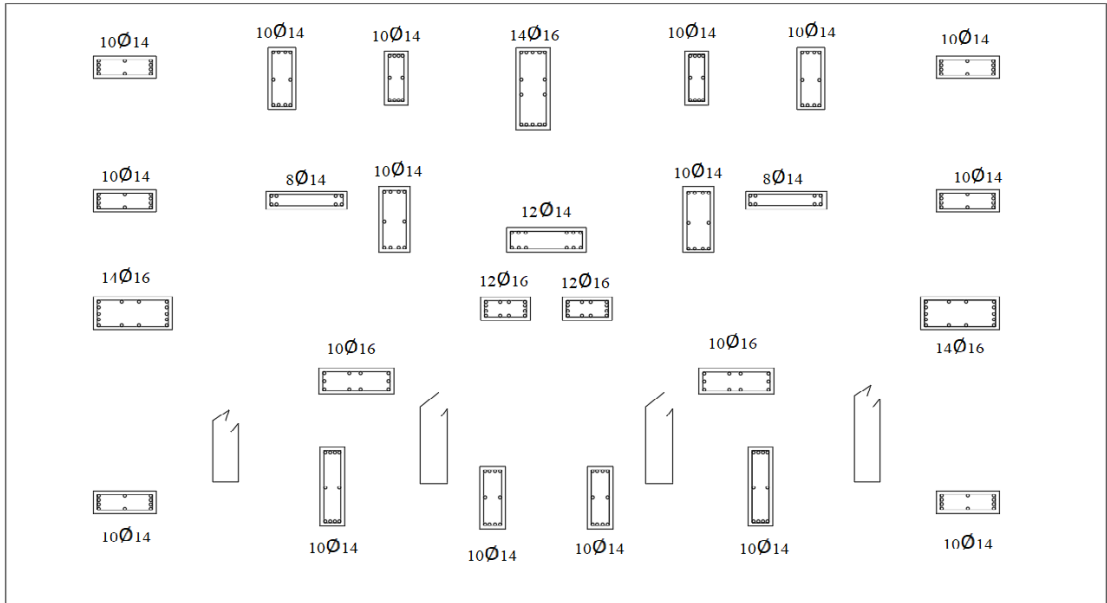


Figure A5: Reinforcement rebar of columns of ground floor

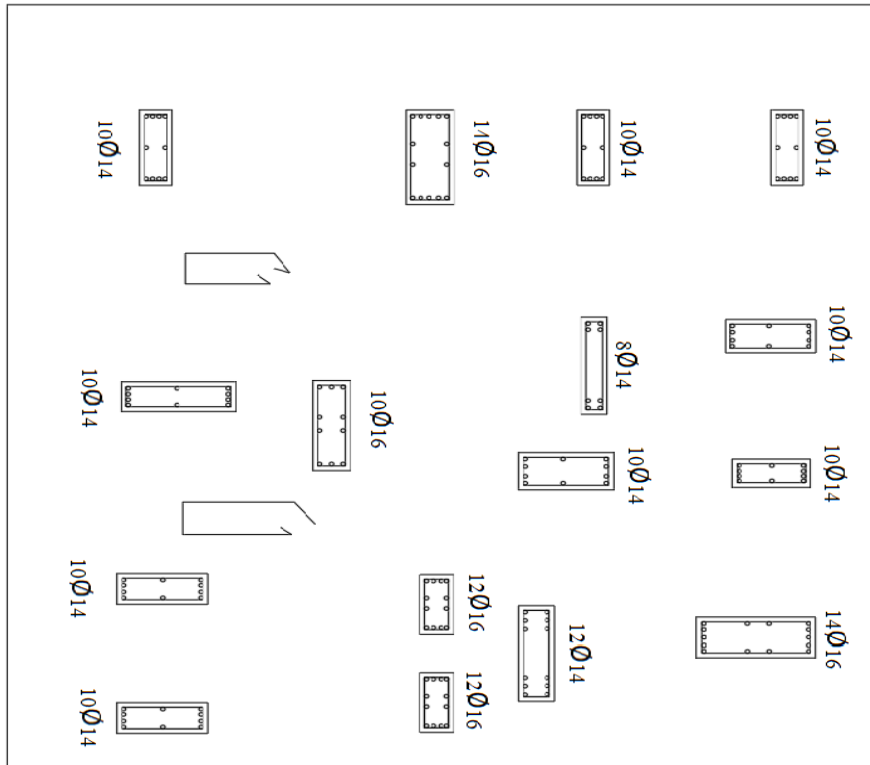


Figure A6: Reinforcement rebar of columns of the first floor

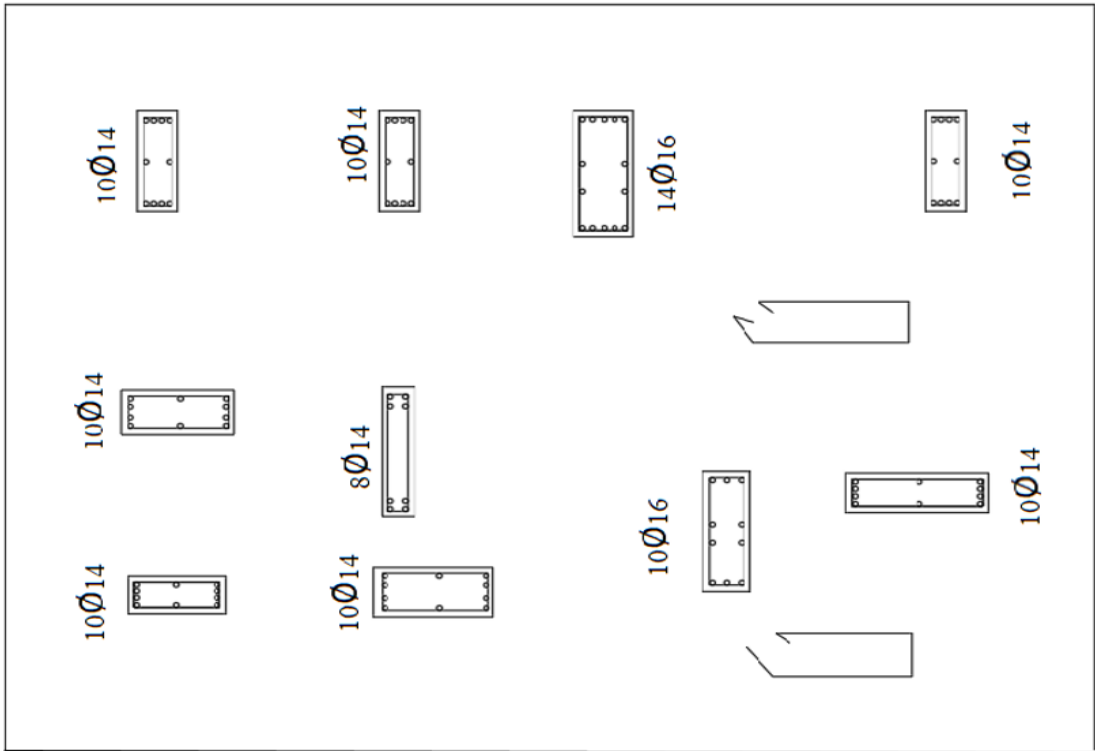


Figure A7: Reinforcement rebar of columns of the first floor

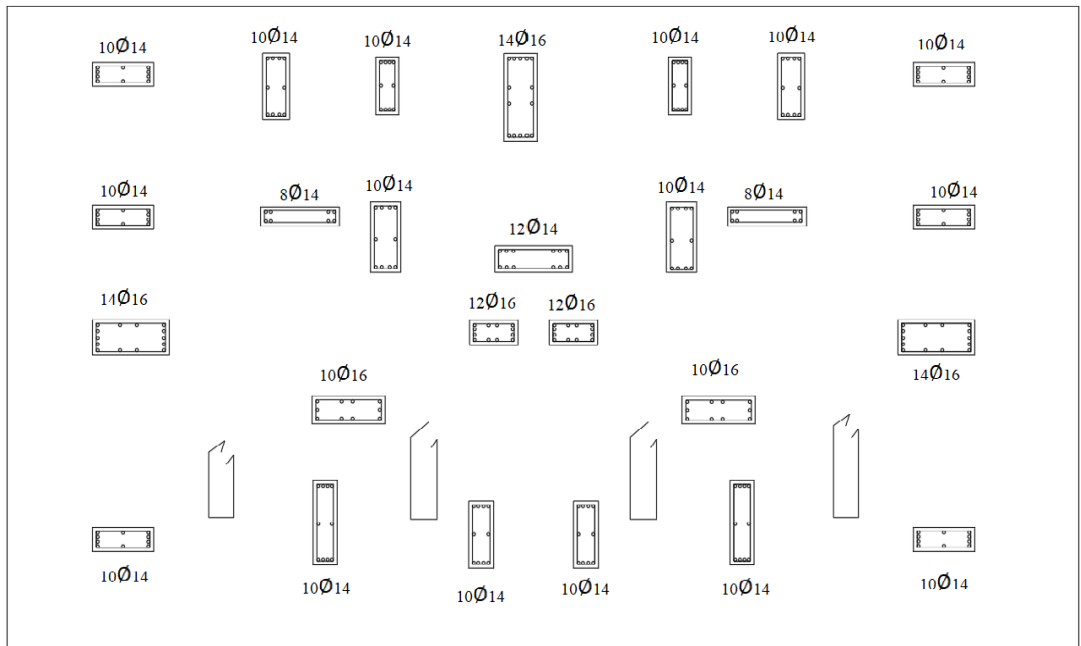


Figure A8: Reinforcement rebar of columns of second, third and fourth floor

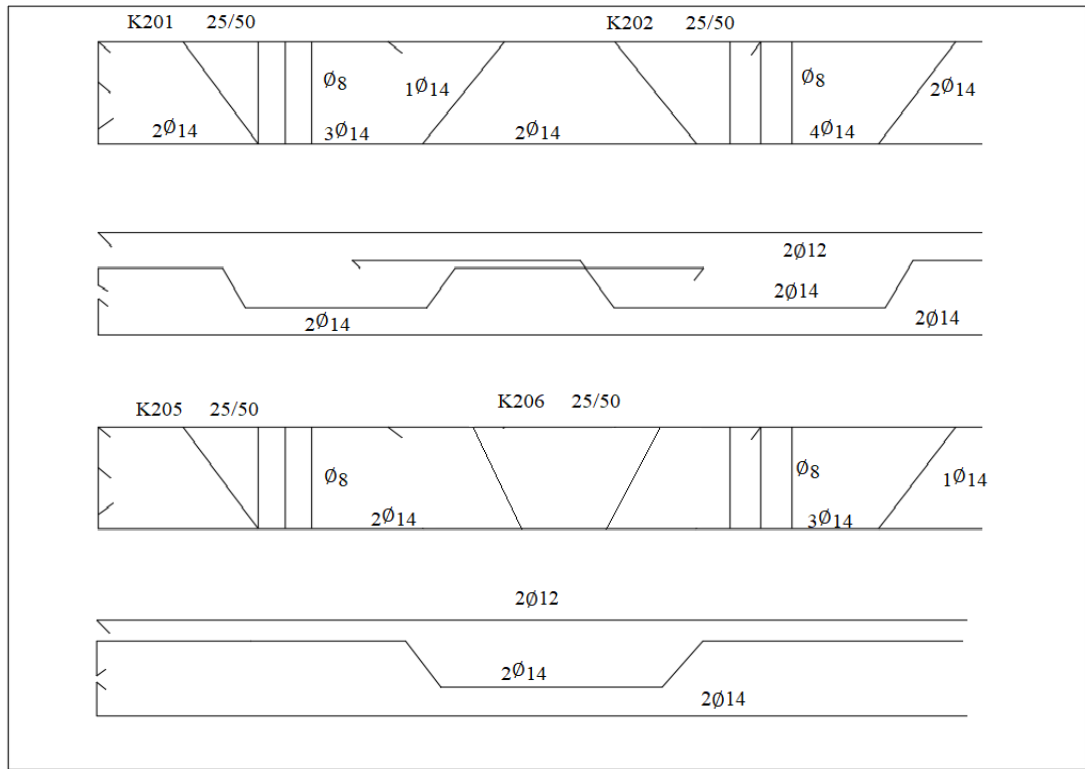


Figure A9: Reinforcement rebar of beams of studied building (K201, K202, K205, and K206)

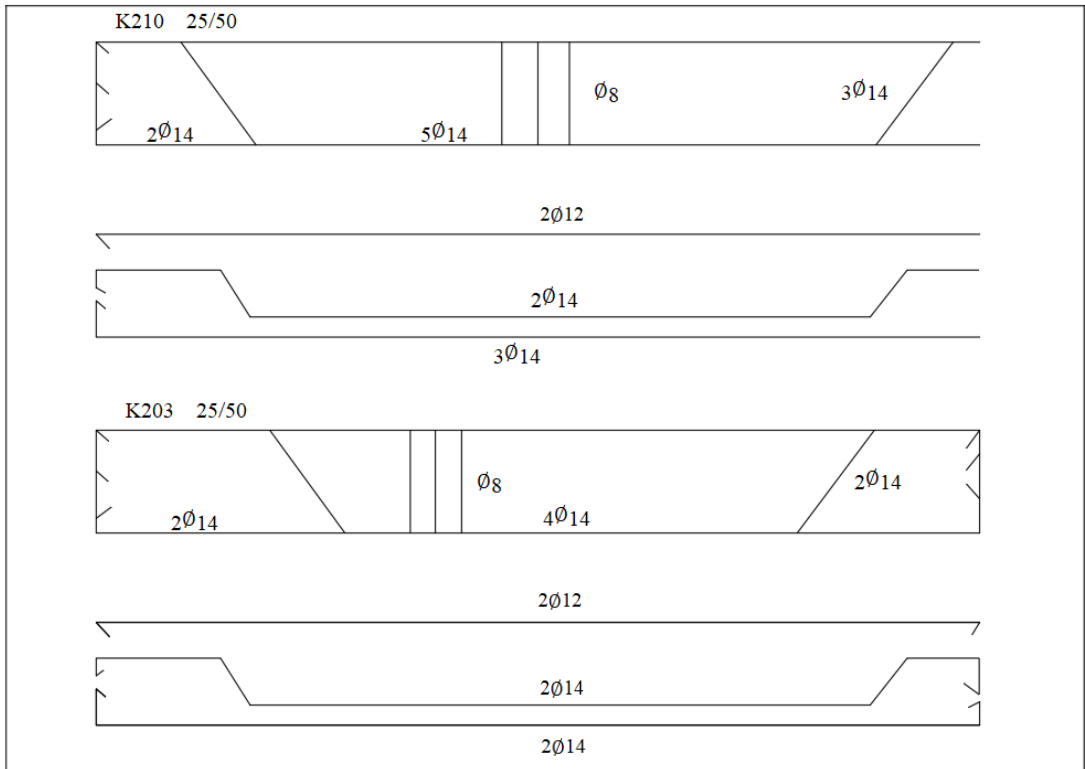


Figure A10: Reinforcement rebar of beams of studied building (K210 and K203)

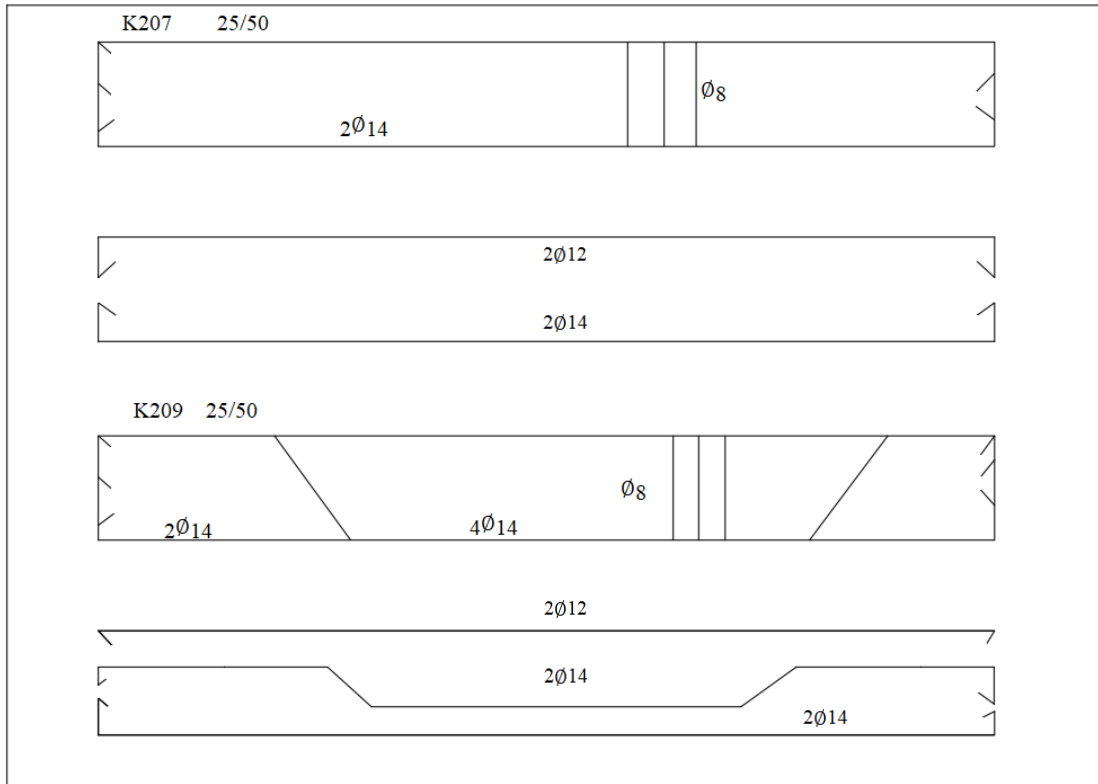


Figure A11: Reinforcement rebar of beams of studied building (K207 and K209)

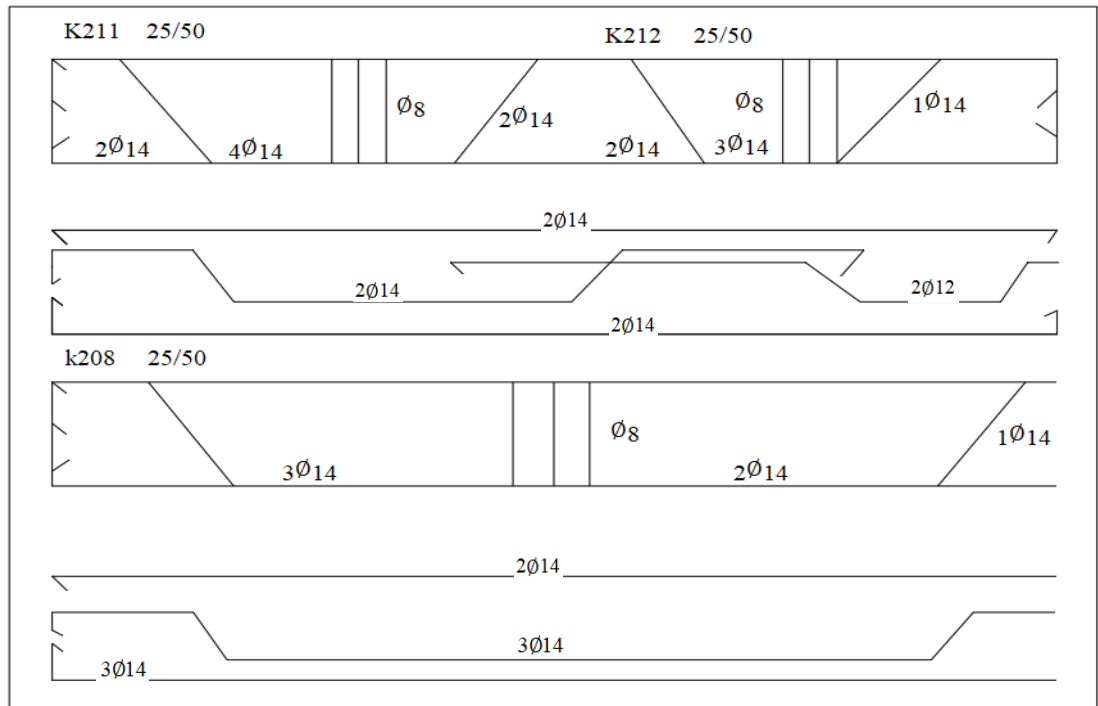
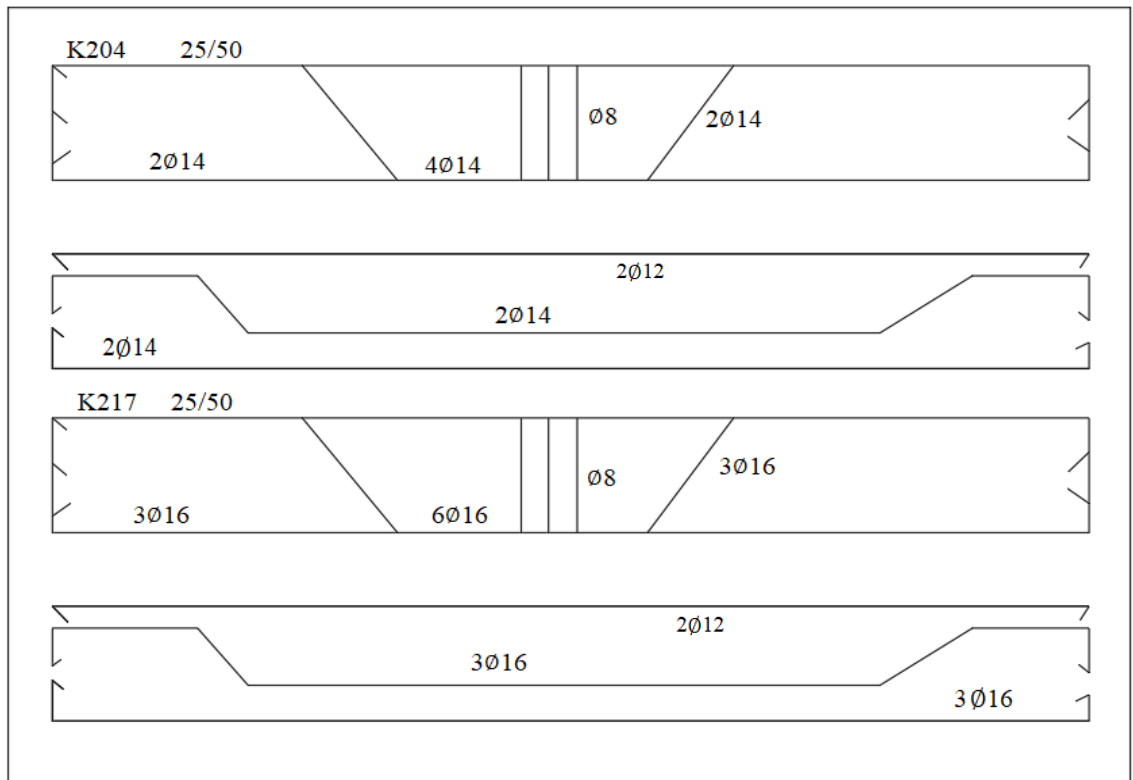
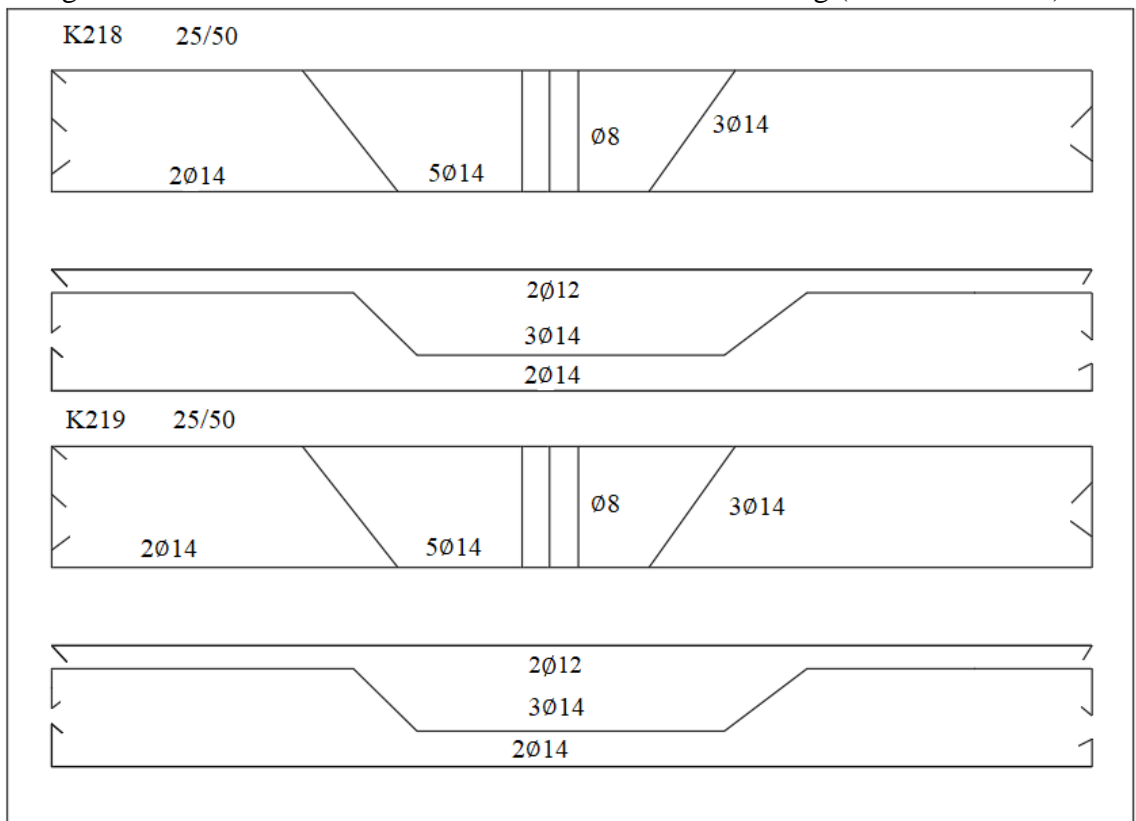


Figure A12: Reinforcement rebar of beams of studied building (K211, K212 and K208)



FigureA13: Reinforcement rebar of beams of studied building (K204 and K217)



FigureA14: Reinforcement rebar of beams of studied building (K18 and K219)

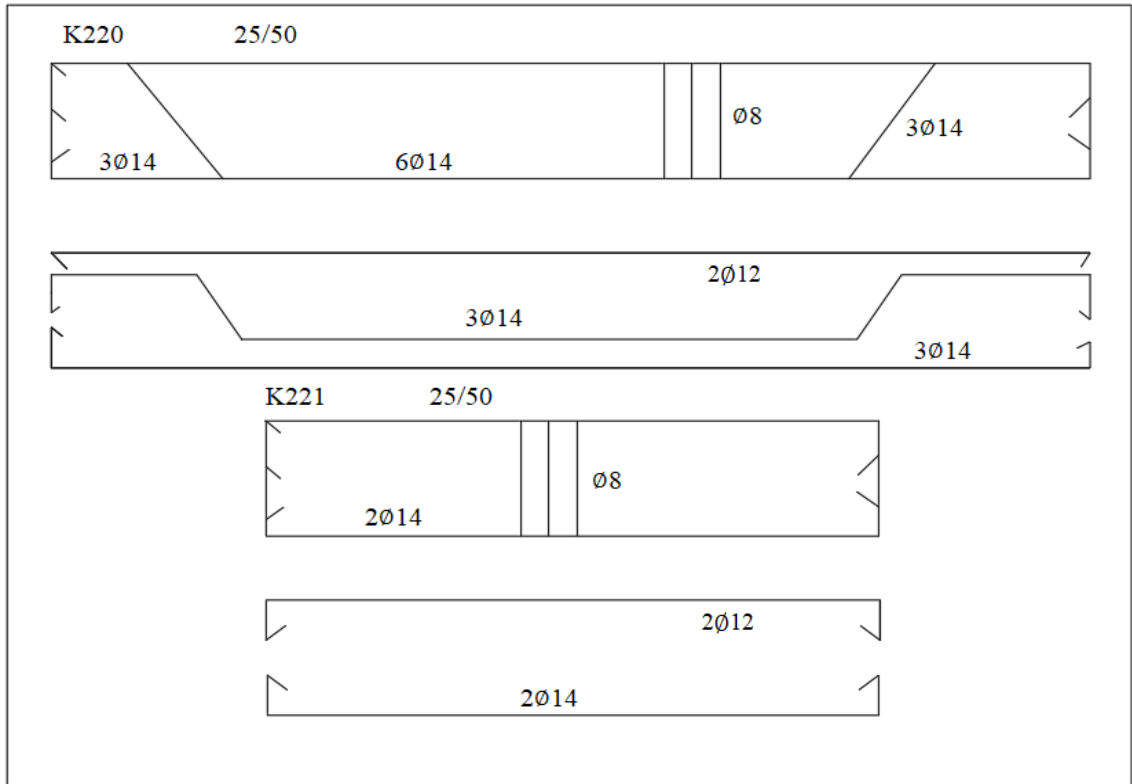


Figure A15: Reinforcement rebar of beams of studied building (K220 and K221)

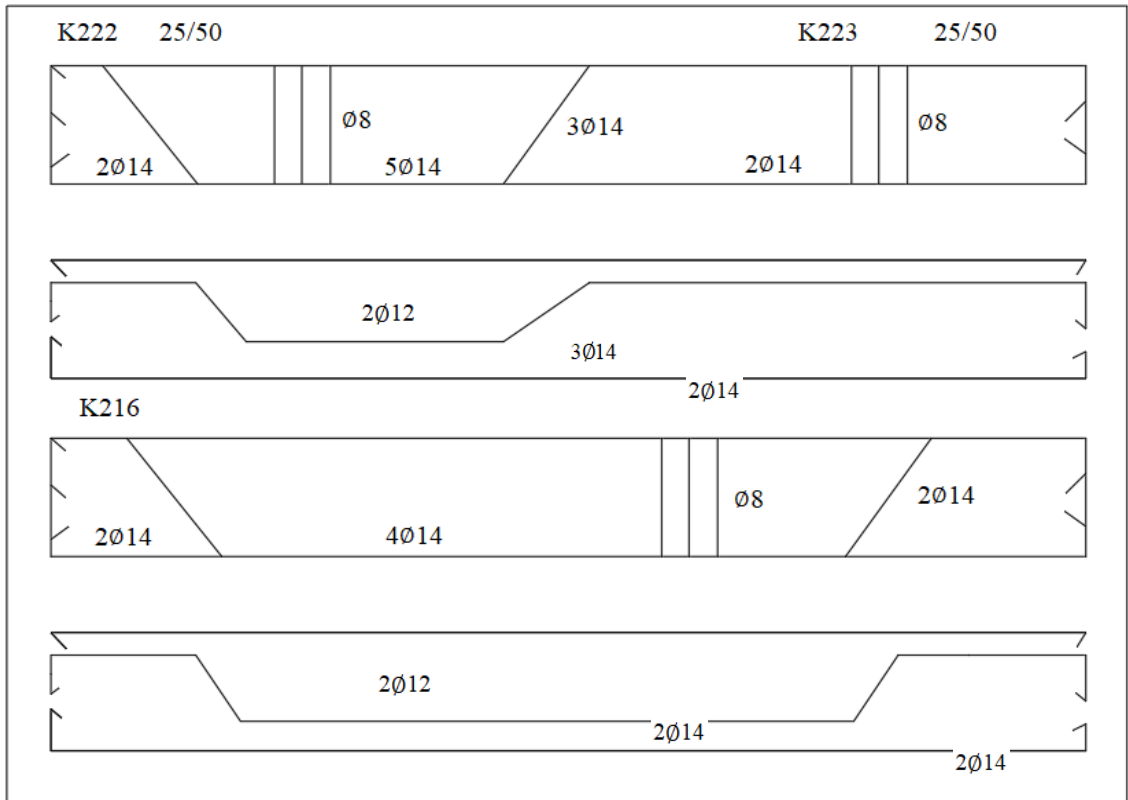


Figure A16: Reinforcement rebar of beams of studied building (K222, K221 and K216)

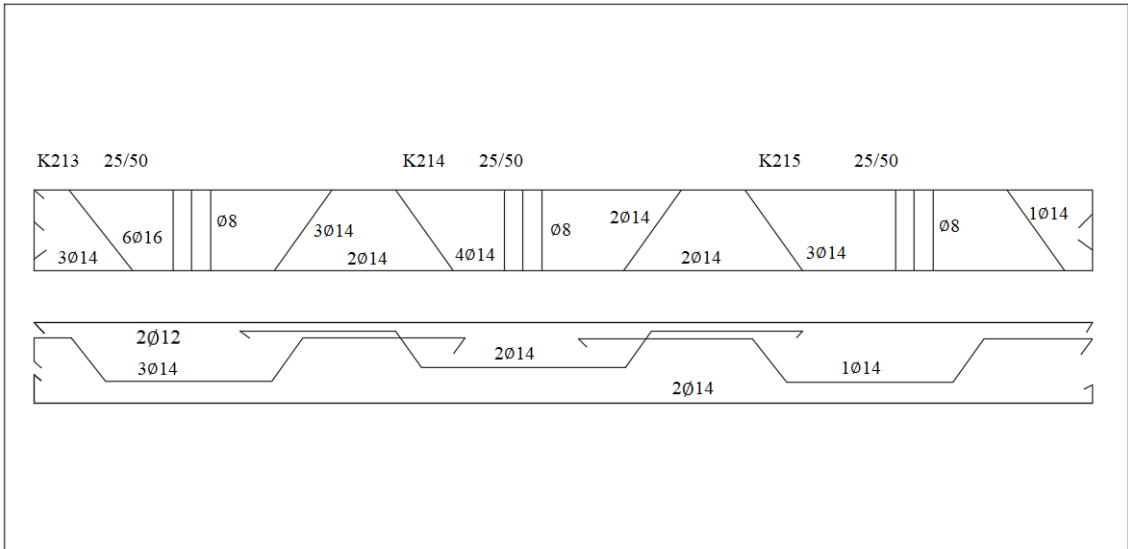


Figure A17: Reinforcement rebar of beams of studied building (K213, K214 and K215)

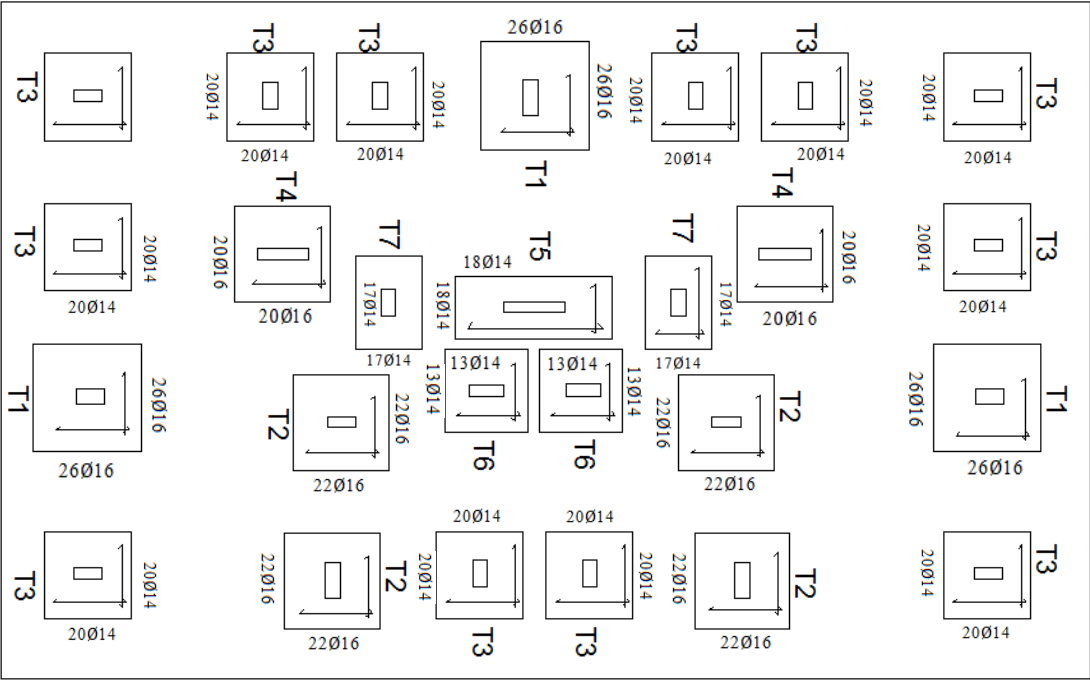


Figure A18: Reinforcement rebar of foundation of studied building (T1, T2, T3, T4, T5, T6 and T7)